Permafrost in Switzerland

2010/2011 to 2013/2014

Glaciological Report (Permafrost) No. 12–15

2016

Permafrost in Switzerland

2010/2011 to 2013/2014

Glaciological Report (Permafrost) No. 12–15

Swiss Permafrost Monitoring Network

Edited by

Jeannette Nötzli, Rachel Lüthi and Benno Staub

PERMOS Office, c/o Department of Geosciences, University of Fribourg

2016

Publication of the Cryospheric Commission of the Swiss Academy of Sciences (SCNAT)

ISSN 2296-6153 (Online)
ISSN 2296-6145 (Print)

Swiss Permafrost Monitoring Network (PERMOS)
c/o Department of Geosciences
University of Fribourg
Chemin du Musée 4
CH–1700 Fribourg
http://www.permos.ch
office@permos.ch

Citation

PERMOS 2016. Permafrost in Switzerland 2010/2011 to 2013/2014. Noetzli, J. , Luethi, R., and Staub, B. (eds.), Glaciological Report Permafrost No. 12–15 of the Cryospheric Commission of the Swiss Academy of Sciences, 85 pp.

Data Set

This report is based on the PERMOS data set published under DOI 10.13093/permos-2016-01 (for meta data and borehole temperatures). The data are available at http://dx.doi.org/10.13093/permos-2016-01.

Cover Page

Photo of the rock glacier Muragl (Upper Engadine) showing the high spatial variability of factors influencing the thermal regime of the subsurface. Photo: J. Nötzli, July 2013.

Imprint

Project Management and Editing
Jeannette Nötzli, Rachel Lüthi and Benno Staub

Authors

Reynald Delaloye	Department of Geosciences, University of Fribourg
Christin Hilbich	Department of Geography, University of Zurich and Department of Geosciences, University of Fribourg
Rachel Lüthi	WSL Institute for Snow and Avalanche Research SLF, Davos
Jeannette Nötzli	Department of Geography, University of Zurich and WSL Institute for Snow and Avalanche Research SLF, Davos
Marcia Phillips	WSL Institute for Snow and Avalanche Research SLF, Davos
Benno Staub	Department of Geosciences, University of Fribourg

Site Maintenance and Data Acquisition (PERMOS Partners)

- Department of Geography, University of Zurich (UZH):
  Isabelle Gärtner-Roer, Stephan Gruber, Andreas Hasler, Christin Hilbich, Jeannette Nötzli, Andreas Vieli, Ingo Völksch
- Department of Geosciences, University of Fribourg (UniFR):
  Reynald Delaloye, Christian Hauck, Christin Hilbich, Martin Hölzle, Benno Staub
- Institute of Earth Sciences, University of Applied Sciences and Arts of Southern Switzerland (SUPSI):
  Cristian Scapozza
- Institute of Earth Surface Dynamics, Faculty of Geosciences and Environment, Univ. of Lausanne (UniL):
  Christophe Lambiel
- Institute for Geotechnical Engineering, ETH Zurich (IGT-ETH):
  Sarah M. Springman
- WSL Institute for Snow and Avalanche Research SLF, Davos (SLF):
  Marcia Phillips

Review
PERMOS Scientific Committee
PERMOS Steering Committee

Summary Translation
Christophe Lambiel (French), Cristian Scapozza (Italian), Gian Darms (Romontsch)

Printed by
Ebnöther Joos AG, print & publishing, CH–8135 Langnau am Albis

Published Reports

The PERMOS concept and annex were approved by the permafrost coordination group on November 18, 1999 and by the Cryospheric Commission (Expertenkommission Kryosphäre EKK; former Glaciological Commission) on January 14, 2000 and were published in 2000. Annual reports on «Permafrost in Switzerland» started in 1999. The reports listed below are available as hardcopy as well as for download on the PERMOS website http://www.permos.ch

Reporting Period	*Report No.*	*Published*
1999/2000	1	2001
2000/2001 and 2001/2002	2/3	2004
2002/2003 and 2003/2004	4/5	2007
2004/2005 and 2005/2006	6/7	2009
2006/2007 and 2007/2008	8/9	2010
2008/2009 and 2009/2010	10/11	2013
2010/2011 to 2013/2014	12–15	2016

Preface

… and it continues! The likely best investigated mountain permafrost site on rock glacier Corvatsch-Murtèl was mentioned in all previous prefaces. The longest temperature series in mountain permafrost measured in a borehole on a rock glacier serves as a role model for education, research and long-term monitoring and will eventually reach 30 years in 2017, that is the typical length of a reference period in climate related studies. The expected lifetime of the installation and the continuous shearing of the rock glacier have however threatened the continuation of the time series and the risk of loosing the borehole steadily increased. The successful re-drilling in summer 2015 some five metres away and the very pleasing high accordance of the new and old time series are therefore great news for the continuation of the Murtèl success story and a milestone for the long-term monitoring of mountain permafrost in the Swiss Alps. The core task of long-term monitoring – but at the same time and without doubt the biggest challenge – is to deliver reliable, robust and comparable measurements of relevant variables from key sites and over decades. The borehole measurements in PERMOS are complemented by distributed terrestrial observations of ground surface temperature, changes in subsurface ice content as well as rock glacier creep velocities to achieve a comprehensive picture of state and changes of permafrost in the Swiss Alps.

A successful and sound long-term climate-related monitoring service has to meet various additional tasks and challenges on which PERMOS has been (and continues to be) working on: a robust data management system with open and easy access to the data, standardization and quality control for both the measurement data and their illustration and interpretation in agreement with international developments, and timely publication of the most important results in an understandable and useful way towards researchers, authorities and the public.

The on-going operationalization of PERMOS to meet these challenges is based on a solid fundament of the experience of more than 15 years of operation, important financial support of the three agreement partners (joint partnership of the Swiss Federal Office of Meteorology and Climatology MeteoSwiss in the framework of GCOS Switzerland, the Swiss Federal Office for the Environment FOEN, and the Swiss Academy for Sciences SCNAT), which also allowed for an enlargement of the PERMOS Office from this year, and – especially – the enduring dedication, motivation and effort of the institutions and people involved. We are currently reworking the reporting strategy and envisage annual and online information on the permafrost monitoring results, which can be complemented by printed summary assessments on longer-term changes. This report is therefore the last one published in this format.

I would like to express my sincere thanks to all people supporting and carrying PERMOS in any way! Let's keep going and continue the PERMOS success story – that we will reach the significant 30 years for the operation of our network, looking at a solid and straightforward but modern and innovative Swiss Permafrost Monitoring Network.

September 2016, Jeannette Nötzli, PERMOS Office

Summary

The present report on permafrost in the Swiss Alps covers the four hydrological years 2010/2011 to 2013/2014, that is the contract period 2011–2014 of the Swiss Permafrost Monitoring Network (PERMOS). State and changes of permafrost in the Swiss Alps are observed based on temperature measurements at the ground surface and at depth, changes in unfrozen water content determined from geophysical surveys, and creep velocities of rock glaciers taken from terrestrial geodetic surveys.

The meteorological conditions were above average warm during the entire period, which includes two years with new records for annual mean air temperatures (2011 and 2014). The hydrological year 2010/2011 was especially warm and dry in winter, spring and late summer/autumn and snow depths in winter were below average. Winter conditions were cold with above-average amounts of snow in the mountains in the following year, spring was warm and in the beginning of summer conditions were again rather cool and wet. Persistent wintery conditions and an extremely sunny summer characterized the hydrological year 2012/2013. Finally, weather conditions in 2013/2014 were very warm throughout most of the year and only interrupted by a cool and wet midsummer. Record snow amounts were registered in the South.

Near-surface temperatures are measured at a large number of locations with varying topographical settings and on different landforms. They are persisting at a high level since the year 2009 and throughout the reporting period, despite the first two rather cold winters. The recorded annual means, however, did not reach the maxima measured in the hot year 2002/2003. Near-surface temperatures measured in steep rock that closely follow air temperature likely reached new records in 2011 and 2014, but time series only date back to 2004. Active layer thickness was determined by interpolation between thermistors in boreholes and increased for most but not all sites during the reporting period. The ground temperatures measured at around 10 and 20 metres depth reveal a warming trend that started in the year 2009 and continued during the four years of observation. In contrast to the near-surface temperatures, thermal conditions at depth are mostly warmer at the end of the 4-year reporting period than after the record year 2002/2003. A corresponding significant decrease of resistivities was measured at all ERT monitoring sites, which points to a decrease in subsurface ice content. The terrestrial surveys reveal distinct inter-annual variations but show a general strong increase towards a new velocity maximum in rock glacier creep velocities at most sites since 2007.

In summary, all elements observed during the reporting period within the PERMOS network show a warming trend in permafrost since the year 2009. This is likely a cumulative effect of continuously warm climate conditions.

Zusammenfassung

Der vorliegende Bericht zum Permafrost in den Schweizer Alpen dokumentiert die vier hydrologischen Jahre 2010/2011 bis 2013/2014 und damit die Vertragsperiode 2011–2014 des Schweizer Permafrostbeobachtungsnetzes PERMOS. Zustand und Veränderungen des Permafrosts in den Schweizer Alpen werden durch folgende Elemente beobachtet: Temperaturmessungen an der Bodenoberfläche und im Untergrund, Änderungen des Anteils an ungefrorenem Wasser abgeleitet aus geophysikalischen Untersuchungen und Kriechgeschwindigkeiten der Blockgletscher bestimmt durch terrestrische geodätische Vermessung.

Die meteorologischen Bedingungen waren überdurchschnittlich warm während der gesamten Berichtsperiode, welche auch zwei Jahre mit neuen gemessenen Rekorden der mittleren jährlichen Lufttemperatur umfasst (2011 und 2014). Das hydrologische Jahr 2010/2011 war im Winter, Frühling und Spätsommer/Herbst besonders warm und trocken und die Schneemengen im Winter waren unterdurchschnittlich. Im folgenden Jahr war der Winter kalt mit überdurchschnittlichen Schneemengen in den Bergen. Der Frühling war warm, aber der Sommerbeginn wiederum kühl und nass. Für das hydrologische Jahr 2012/2013 wurden anhaltend winterliche Verhältnisse und ein extrem sonniger Sommer beobachtet. Die Witterungsbedingungen für 2013/2014 waren schliesslich fast das ganze Jahr hindurch warm und wurden nur durch einen kühlen und nassen Hochsommer unterbrochen. Im Süden wurden zudem neue Rekordschneemengen gemessen.

Die Temperaturen nahe der Oberfläche werden an vielen Standorten mit unterschiedlichen topographischen Bedingungen und auf verschiedenen Landformen gemessen. Seit dem Jahr 2009 und während der ganzen Berichtsperiode bleiben sie auf einem hohen Niveau. Die Jahresmittel erreichten aber die im Jahr 2002/2003 gemessenen Rekordwerte nicht. Die Oberflächentemperaturen im steilen Fels, die sehr stark der Lufttemperatur folgen, erreichten in 2011 und 2014 vermutlich neue Rekordwerte. Die Zeitreihen gehen aber nur bis 2004 zurück. Die Tiefe der Auftauschicht wird mittels Interpolation zwischen Thermistoren in Bohrlöchern bestimmt und hat in der Berichtsperiode an den meisten, aber nicht allen Standorten zugenommen. Die Temperarturen im Untergrund, die in Tiefen von 10 und 20 Metern gemessen werden, zeigen seit 2009 einen Erwärmungstrend, der sich auch in den vier Berichtsjahren fortsetzte. Im Gegensatz zu den Oberflächentemperaturen sind die Untergrundtemperaturen am Ende der Berichtsperiode mehrheitlich höher als nach dem Rekordjahr 2002/2003. Dazu passend zeigen die geophysikalischen Messungen eine signifikante Abnahme der elektrischen Widerstände, was auf eine Abnahme an Untergrundeis hinweist. Die geodätische Vermessung zur Bestimmung der Blockgletschergeschwindigkeiten zeigen deutliche Unterschiede zwischen den Jahren, aber generell für die meisten Standorte einen starken Anstieg der Kriechgeschwindigkeiten zu einem neuen Maximum seit 2007.

Zusammenfassend zeigen alle in der Berichtsperiode beobachteten Elemente im PERMOS-Messnetz einen Erwärmungstrend im Permafrost seit dem Jahr 2009. Dieser ist wahrscheinlich ein kumulatives Resultat der anhaltend warmen Witterungsbedingungen.

Resumé

Ce rapport sur le pergélisol dans les Alpes Suisses couvre les quatre années hydrologiques 2010/2011 à 2013/2014, qui correspond à la période de contrat 2011–2014 du Réseau Suisse de Monitoring du Pergélisol PERMOS. L'état et les changements du pergélisol dans les Alpes Suisses sont documentés à partir des éléments suivants : mesures de la température à la surface du sol et en profondeur, changements dans la teneur en eau non gelée déterminés à partir de mesures géophysiques, vitesses de fluage de glaciers rocheux mesurées par mesures terrestres géodésiques.

Les conditions météorologiques ont été caractérisées par des températures supérieures à la normale durant la période entière, avec deux années présentant de nouveaux records de moyenne annuelle des températures (2011 et 2014). L'année hydrologique 2010/2011 fut spécialement chaude et sèche en hiver, au printemps, à la fin de l'été et en automne et les hauteurs de neige en hiver furent en dessous de la norme. Durant l'année suivante, les conditions hivernales furent froides, avec des hauteurs de neige en montagne supérieures à la norme. Le printemps fut chaud et le début de l'été fut à nouveau plutôt frais et humide. Des conditions hivernales persistantes et un été extrêmement ensoleillé caractérisèrent l'année hydrologique 2012/2013. Finalement, les conditions météorologiques en 2013/2014 furent très chaudes tout au long de l'année et furent seulement interrompues par un milieu d'été frais et humide. Des quantités de neige record furent enregistrées au Sud.

Les températures de la proche surface sont mesurées sur un grand nombre de sites dans différents contextes topographiques et sur différents types de formes géomorphologiques. Elles sont élevées depuis 2009 et le sont restées tout au long de la période rapportée, malgré les deux premiers hivers plutôt frais. Les moyennes annuelles n'ont toutefois pas atteint les maximas enregistrés durant l'année chaude 2002/2003. Les températures de la proche surface mesurées dans les parois rocheuses, qui suivent de manière très proche les températures de l'air, ont atteint de nouveaux records en 2011 et 2014. Le début des mesures n'a toutefois débuté qu'en 2004. L'épaisseur du niveau actif est déterminée par interpolation entre thermistors dans des forages. Elle augmenta dans une grande partie des cas au cours de la période reportée. Les températures mesurées en profondeur à environ 10 et 20 mètres montrent une tendance au réchauffement qui débuta durant l'année 2009 et qui perdura durant les quatre années d'observation. Contrairement à la proche surface, les conditions thermiques en profondeur furent globalement plus chaudes à la fin de la période reportée qu'après l'année record 2002/2003. Une diminution significative des résistivités fut mesurée sur tous les sites de monitoring ERT, ce qui témoigne d'une diminution de la teneur en glace dans le sous-sol. Bien que les mesures de vitesses des glaciers rocheux révèlent d'importantes variations interannuelles, elles montrent globalement une forte accélération qui tend vers de nouvelles vitesses maximales sur la plupart des sites depuis 2007.

En résumé, tous les éléments observés durant la période reportée au sein du réseau PERMOS montrent une tendance au réchauffement du permafrost depuis l'année 2009. Il s'agit vraisemblablement d'un effet cumulé de conditions climatiques chaudes et continuelles.

Riassunto

Questo rapporto sul permafrost nelle Alpi svizzere copre i quattro anni idrologici dal 2010/2011 al 2013/2014, corrispondenti al periodo di contratto 2011–2014 della Rete Svizzera di Monitoraggio del Permafrost PERMOS. Lo stato e i cambiamenti del permafrost nelle Alpi svizzere sono osservati sulla base di misure di temperatura alla superficie del suolo e in profondità, di variazioni della resistività elettrica determinate da prospezioni geofisiche, e di velocità di reptazione dei ghiacciai rocciosi derivate da misurazioni geodetiche terrestri.

Le condizioni meteorologiche sono state superiori al riscaldamento medio durante l'intero periodo, che include due anni con nuovi record per le temperature medie annue dell'aria (2011 e 2014). L'anno idrologico 2010/2011 è stato particolarmente caldo e secco in inverno, primavera e tarda estate/autunno, mentre le altezze della neve in inverno sono state inferiori alla media. Le condizioni invernali sono state fredde, con quantitativi di neve sopra la media in montagna nell'anno seguente. La primavera è stata calda e l'inizio dell'estate è stato nuovamente caratterizzato da condizioni fredde e umide. Condizioni invernali persistenti ed estati estremamente soleggiate hanno caratterizzato l'anno idrologico 2012/2013. Per terminare, le condizioni meteorologiche durante il 2013/2014 sono state molto calde durante buona parte dell'anno, interrotte solamente da un periodo più freddo e umido al cuore dell'estate. Nuovi quantitativi record di innevamento sono stati registrati al Sud delle Alpi.

Le temperature a prossimità della superficie del suolo sono misurate in una moltitudine di siti variando la posizione topografica e su forme geomorfologiche differenti. Queste si mantengono su valori elevati sin dal 2009 e durante tutto il periodo coperto da questo rapporto, fatta eccezione dei primi due inverni, moderatamente freddi. Le medie annue registrate, tuttavia, non hanno raggiunto il valore massimo misurato durante l'anno molto caldo 2002/2003. Le temperature a prossimità della superficie misurate nelle pareti rocciose hanno seguito strettamente le temperature dell'aria, stabilendo nuovi record nel 2011 e nel 2014, ma con la serie storica delle misure che risale solamente al 2004. Gli spessori dello strato attivo sono stati determinati dall'interpolazione dei dati dei sensori di temperatura nelle perforazioni. Essi sono aumentati per quasi tutti i siti per il periodo coperto dal presente rapporto. Le temperature del suolo misurate a una profondità compresa tra 10 e 20 metri rivelano una tendenza al riscaldamento iniziata nel 2009 e continua lungo tutti e quattro gli anni di misurazioni. Al contrario della superficie del suolo, le condizioni termiche in profondità sono molto più calde alla fine del periodo 2010/2011–2013/2014 rispetto a quanto misurato a seguito dell'anno record 2002/2003. Una diminuzione significativa delle resistività elettriche è quindi di conseguenza stata misurata in tutti i siti di monitoraggio ERT, indicando una diminuzione nel contenuto di ghiaccio nel sottosuolo. Le misurazioni geodetiche terrestri hanno rivelato delle variazioni inter-annuali ben distinte, anche se in molti siti è possibile osservare una tendenza generale verso un nuovo record delle velocità di reptazione dei ghiacciai rocciosi dal 2007.

In conclusione, tutti i parametri osservati dalla rete PERMOS durante il periodo coperto da questo rapporto mostrano una tendenza al riscaldamento del permafrost in atto dal 2009. Questo è dovuto molto probabilmente all'effetto cumulato di una successione di condizioni climatiche calde.

Resumaziun

Quest rapport pertucont la schelira permanenta en las Alps svizras cuviera ils quater onns hidrologics 2010/2011 tochen 2013/2014. Quei ei la perioda da contract 2011–2014 dalla reit svizra per la survigilonza dalla schelira permanenta (PERMOS). Stadis e midadas dalla schelira permanenta en las Alps svizras vegnan observai cun mesiraziuns dalla temperatura alla surfatscha dil terren ed a funs, midadas dalla resistenza electrica determinada sin retschercas geofisicalas sco era cun mesiraziuns dalla spertadad dil ruschnar dalla schelira permanenta sin basa da retschercas geodeticas terrestras.

Las cundiziuns meteorologicas eran caracterisadas da temperaturas sur la media duront igl entir temps. En dus onns ha ei dau novs records dallas temperaturas medias annulas (2011 e 2014). 2010/2011 eran igl unviern, la primavera sco era la fin dalla stad/igl atun schetgs e specialmein caulds, las altezias da neiv era sut la media. Duront igl onn suivont ha ei fatg freid cun altezias da neiv sur la media ellas muntognas. La primavera ha ei fatg cauld ed all'entschatta dalla stad ei l'aura bletscha e freida turnada. Relaziuns invernalas d'in cuntin ed ina stad fetg sulegliva han caracterisau igl onn hidrologic 2012/2013. Per finir ein las cundiziuns meteorologicas egl onn 2013/2014 stadas plitost cauldas duront la gronda part digl onn. Mo da mesa stad eisi stau cuort freid e bletsch. El sid hai ei dau novs records tgei che appartegn las altezias da neiv.

Las temperaturas datier dalla surfatscha vegnan mesiradas en numerus loghens cun variontas cundiziuns dalla topografia e differentas fuormas dalla cuntrada. Dapi 2009 ein quellas temperaturas persistentamein sin in ault livel, dispet ils emprems dus unviarns plitost freids. Las medias annualas han denton buc contonschiu las valurs maximalas ch'ins ha mesirau egl onn cauld 2002/2003. Las temperaturas dalla surfatscha en preits crap che suondan pli u meins la temperatura dall'aria han carteivlamein contonschiu novs records 2011 e 2014. Quellas mesiraziuns dat ei denton mo dapi 2004. La grossezia dalla cozza activa ei vegnida interpolada sin basa da mesiraziuns da temperatura ella fora da sondagi. La grossezia ei augmentada tier bunamein tut ils loghens duront la perioda d'examinaziun. Las temperaturas dil terren en ina profunditad da 10 e 20 meters muossan ina tendenza tier temperaturas pli cauldas, la quala ha entschiet egl onn 2009 e continuau en la perioda examinada da quest rapport. Cuntrari allas temperaturas datier dalla surfatscha ein quellas pli profundas per gronda part pli aultas suenter questa perioda da quater onns che suenter igl onn da record 2002/2003. Las observaziuns dalla resistivitad ein – adequatamein a quei fatg – significantamein pli bassas tier tut ils loghens da monitoring ERT. Quei indichescha ina sminuaziun el cuntegn da glatsch datier dalla surfatscha. Las retschercas terrestras muossan distinctas variaziuns duront ils onns da mesiraziun. Denton dat ei en general ina ferma augmentaziun en direcziun dad in niev maximum da spertadad els moviments dils glatschers cumpacts tier ils pli biars loghens dapi 2007.

Resumond ils fatgs san ins dir che tut ils elements d'observaziun ella reit da PERMOS indicheschan in trend en direcziun da temperaturas pli aultas ella schelira permanenta dapi igl onn 2009. Quei ei pli probabel in effect cumulativ dallas cundiziuns climaticas pli cauldas.

Contents

1 Introduction

This report on permafrost in the Swiss Alps covers the four hydrological years 2010/2011 to 2013/2014 and the contract period 2011–2014 of the Swiss Permafrost Monitoring Network PERMOS. It is the 6th of its kind, but the first to report on four years. The official PERMOS operation and reporting started with the first pilot phase in the year 2000.

PERMOS relies on substantial financial support by the joint partnership of the Swiss Federal Office of Meteorology and Climatology MeteoSwiss in the framework of GCOS Switzerland, the Swiss Federal Office for the Environment (FOEN), and the Swiss Academy for Sciences (SCNAT). PERMOS is run by its coordinating office, the PERMOS Office, six partner institutions and a Steering and Scientific Committee, and it is part of the Swiss cryosphere monitoring (www.cryosphere.ch). Within the international framework, PERMOS is one of the early components of the Global Terrestrial Network for Permafrost (GTN-P) of the worldwide climate-monitoring program GCOS (Global Climate Observing System, a joint undertaking of the World Meteorological Organization WMO, the Intergovernmental Oceanographic Commission IOC of the United Nations Educational Scientific and Cultural Organization UNESCO, the United Nations Environment Programme UNEP and the International Council for Science ICSU). Within the five-tiered principle proposed for the Global Hierarchical Observing Strategy (GHOST, cf. Harris et al. 2001 for adaptation to permafrost observation) the national network mainly contributes to tiers 3 and 4. It provides observations to sample the range of environmental variation in permafrost thermal state as in tier 3 (regional observations at intermediate depths and regular time intervals) and aims to describe representative permafrost conditions based on the observation sites and elements as in tier 4 (ground thermal conditions to provide representative permafrost conditions).

Permafrost is a thermal phenomenon of the subsurface. The connection between climate and subsurface thermal regime is not straightforward because snow conditions, surface and subsurface characteristics, subsurface ice, and mountain topography can alter or mask changes in atmospheric conditions (Chapter 2) when they propagate into the subsurface. The strategy to observe mountain permafrost in the Swiss Alps therefore follows a «landform-based approach»: That is, differences in the subsurface thermal regime due to varying climate conditions in Switzerland are considered to be smaller than those caused by topography or surface and subsurface conditions of the different landforms (Figure 1.1). The main landforms distinguished are rock walls (e.g., Eiger North Face), crests (e.g., Matterhorn-Hörnligrat, Schilthorn, Stockhorn), talus slopes (e.g., Les Attelas, Lapires, Muot da Barba Peider), and rock glaciers (e.g., Corvatsch-Murtèl, Réchy, Schafberg). The measurements focus on three observation elements in order to capture these features: (1) ground-surface and subsurface temperatures, (2) changes in relative ice content, and (3) permafrost creep velocities. The three elements complement each other in order to deliver a comprehensive picture of permafrost state and changes in the Swiss Alps.

The core of the network are subsurface or ground temperatures (GT) measured in boreholes, which provide direct evidence of permafrost and its changes (Figure 1.2, Chapter 3). Temperature changes at depth integrate and filter the signal from the surface and reflect trends with a delay, but more clearly. They are however often influenced by 3D effects of the mountain topography and latent heat. For temperatures just below the melting point, phase changes absorb energy and only small or no changes can be observed. Temperature measurements at or near the ground surface (GST) around a borehole or on rock glaciers capture the spatial variability at the

Figure 1.1: *Photo of the rock glacier Muragl showing the high spatial variability over short distance of factors influencing the thermal regime of the subsurface, such as snow conditions, slope and slope exposition, surface characteristics or subsurface ice. Photo: J. Nötzli, July 2013.*

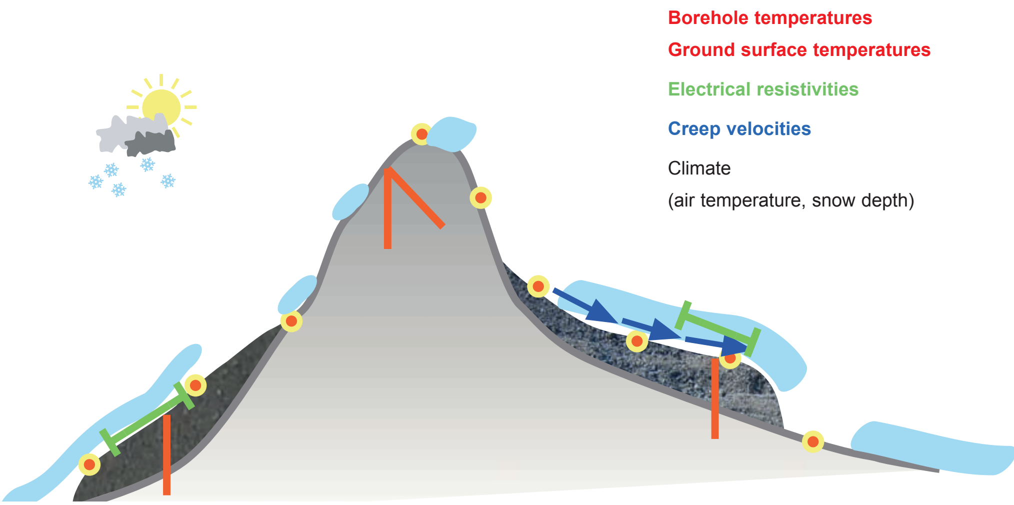

Figure 1.2: *Schematic sketch of the PERMOS observation strategy, which builds on terrestrial measurements of ground temperatures at the surface and at depth, changes of electrical resistivities and creep velocities of rock glaciers at sites with differing topographic settings and landform characteristics.*

Table 1.1: Overview of the PERMOS sites, their main morphology and the type(s) of terrestrial measurements carried out. Sites are sorted alphabetically and reference sites are marked in bold. BH=borehole, GST=ground surface temperature, RST=rock surface temperature, ERT=electrical resistivity tomography, TGS=terrestrial geodetic survey.

Site	Institute(s)	Region	Morphology	BH	GST	RST	ERT	TGS
Aget	UniFR	Lower Valais	Rock glacier		x			x
Alpage de Mille	UniFR	Lower Valais	Rock glacier		x			x
Corvatsch-Murtèl	UZH	Engadine	Rock glacier	x	x	x	x	x
Dreveneuse	UniFR	Chablais	Talus slope	x	x			
Flüela	SLF	Engadine	Talus slope	x				
Gemmi-Furggentälti	UniFR	Upper Valais	Rock glacier		x			x
Gentianes	UniL	Lower Valais	Moraine	x	x			
Gemsstock	SLF	Urner Alps	Crest	x				
Grosses Gufer	UniFR	Upper Valais	Rock glacier		x			x
Jungfraujoch	SLF/UZH	Bernese Oberland	Crest	x		x		
Lapires	UniL/UniFR	Lower Valais	Talus slope	x	x		x	x
Les Attelas	UniL	Lower Valais	Talus slope	x	x		x	
Matterhorn	SLF	Upper Valais	Crest	x				
Monte Prosa	UniFR	Ticino	Rock glacier		x			x
Muot da Barba Peider	SLF	Engadine	Talus slope	x				
Muragl	ETH/UZH	Engadine	Rock glacier	x				x
Réchy	UniFR	Lower Valais	Rock glacier		x	x		x
Ritigraben	SLF	Upper Valais	Rock glacier	x				
Schilthorn	UZH	Bernese Oberland	Crest	x	x	x	x	
Schafberg	SLF	Engadine	Rock glacier	x	x			
Stabbio di Largario	SUPSI	Ticino	Rock glacier		x			x
Stockhorn	UniFR	Upper Valais	Crest	x			x	
Tsarmine	UniL/UniFR	Lower Valais	Rock glacier		x			x
Tsaté	UniL	Lower Valais	Crest	x	x			
Turtmanntal-Hungerlitälli	UZH	Upper Valais	Rock glacier		x			x
Valle di Sceru	SUPSI	Ticino	Rock glacier		x			x
Yettes Condjà	UniL	Lower Valais	Rock glacier		x			x

scale of a landform and allow for the examination of the influence of different surface cover types, topographic settings and snow characteristics on the ground thermal regime.

Electrical resistivity tomography (ERT) monitoring are performed at selected borehole sites (Chapter 4). Based on the differing electrical resistivities of frozen and unfrozen ground material and the changes observed between different surveys, the relative changes in unfrozen water content and subsurface ice are calculated.

It has been observed across the European Alps that with increasing ground temperature, the creep velocities of rock glaciers (as well as other permafrost creep features) also increase. Therefore, the movement of rock glaciers is observed based on at least annual terrestrial geodetic surveys (TGS) of a number of points on each landform (Chapter 5). Air photos taken at these sites allow the observation of creep velocities by photogrammetric analyses. Fast mass movements from permafrost areas (rock fall events) are also documented.

The PERMOS network currently includes 16 sites where GT and GST are observed (Table 1.1, Figure 1.4). ERT is performed at five of these sites. Terrestrial surveys, GST and regular air photos are taken on 14 rock glaciers (Figures 1.3 and 1.5). The sites have been evaluated by the PERMOS Scientific Committee in 2007 and in 2009 based on their relevance, feasibility and scientific and societal interest. Sites where long-term monitoring is most reasonable and feasible have been designated as «PERMOS reference sites». They build the corner stones of the network and are treated with priority.

The field work and site maintenance of the PERMOS network are carried out by the PERMOS partner institutes:

- ETH Zurich: Institute for Geotechnical Engineering (IGT–ETH)
- Univ. of Applied Sciences and Arts of Southern Switzerland, Institute of Earth Sciences (SUPSI)
- Univ. of Fribourg: Department of Geosciences (UniFR)
- Univ. of Lausanne: Faculty of Geosciences and Environment, Institute of Earth Surface Dynamics (UniL)
- Univ. of Zurich: Department of Geography, Glaciology, Geomorphodynamics & Geochronology (UZH)
- WSL Institute for Snow and Avalanche Research SLF, Davos (SLF)

Figure 1.3: View on the Becs de Bosson rock glacier (Val de Réchy, VS). Photo: B. Staub.

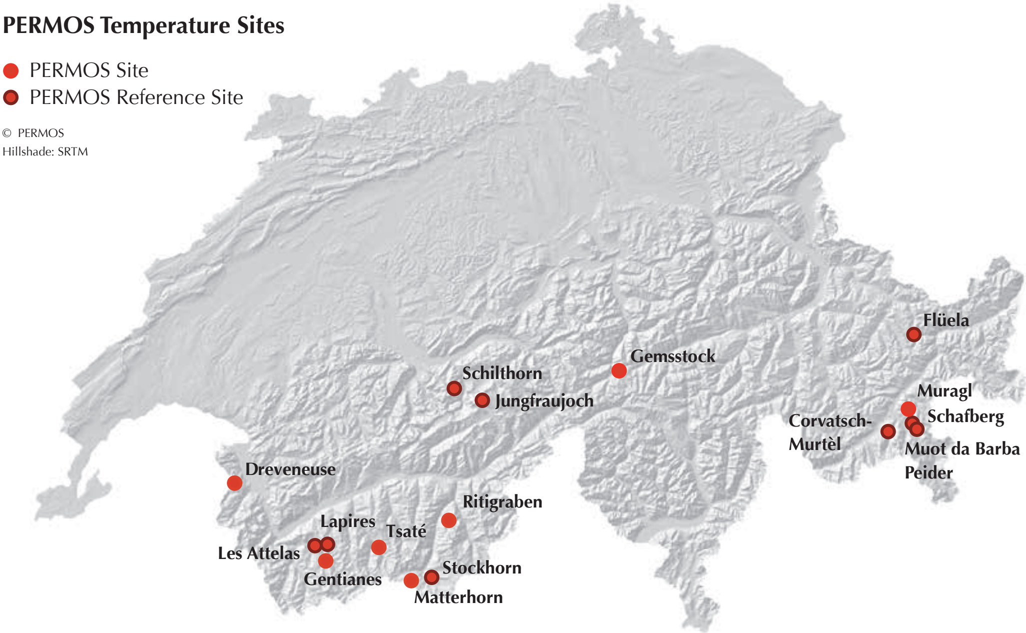

Figure 1.4: *PERMOS temperature sites.*

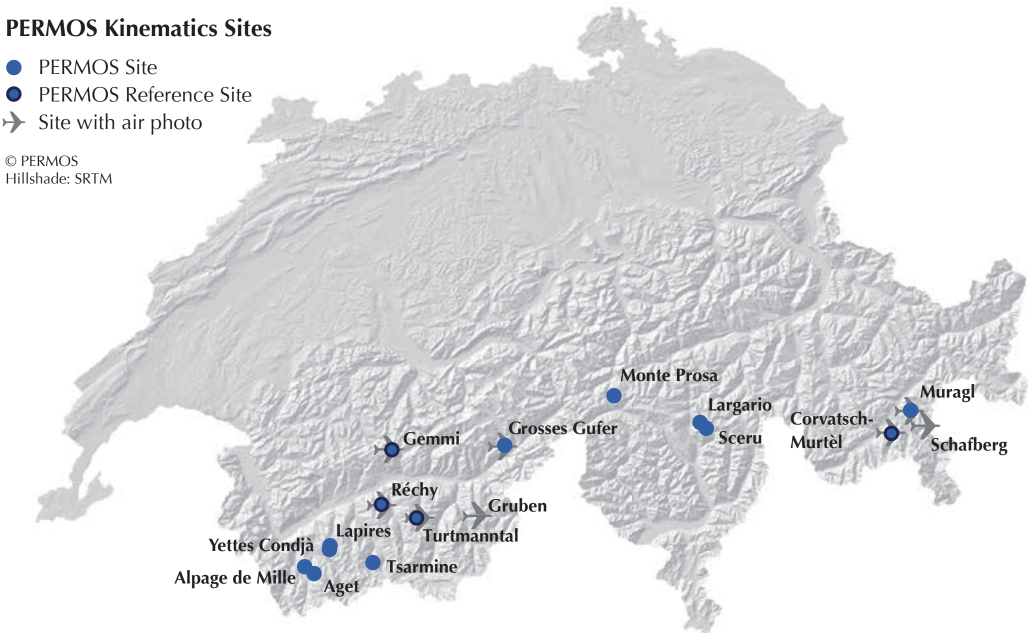

Figure 1.5: *PERMOS kinematics sites.*

2 Weather and Climate

In this section we describe the weather and climate conditions, which have the most important influence on the inter-annual variations of the ground thermal regime. The general weather and climate information is taken from the reports by MeteoSwiss (MeteoSwiss 2010, 2012, 2013, 2014, 2015) and the snow information is provided by the WSL Institute for Snow and Avalanche Research SLF. Note that the climate norm period used by MeteoSwiss has changed from 1961–1990 to 1981–2010 in 2013. The mean annual temperature 1981–2010 in Switzerland has increased 0.8 °C compared to 1961–1990 and the increase is more pronounced in spring and summer than in fall and winter (Begert et al. 2013).

Air temperature is the driving factor for changes in ground surface temperatures (GST) in periods or areas without a thicker snow cover. A snow cover thermally insulates the ground from the atmospheric conditions. The time of the first snow fall, the duration and thickness of the snow cover and the time when the ground surface becomes snow free in spring are therefore relevant. Some of these parameters can be determined based on continuous GST data (cf. Chapter 3): the percolation of melt water provokes a sudden increase to 0 °C at the time when the snow cover is wet down to its base (start of the zero curtain). Then, GST remain almost stable until the terrain becomes snow free.

2.1 Air Temperatures and Snow Cover in 2010/2011

The meteorological conditions 2010/2011 were characterized by cold conditions from mid-November until the end of December 2010, an above average warm January and February 2011, the warmest spring since 1864, a cool first half of July, and a warm late summer. The year 2011 was the warmest year since 1864 with 2 °C above the mean temperature of the period 1961–1990.

Winter 2010/2011 was much dryer and warmer than normal. Snow depths were lower than average in most areas of the Swiss Alps other than the upper Engadine, northern Tessin and in the south of Graubünden, where they were average (Figures 2.1 and 2.2). First large snowfalls occurred in October and November 2010. December 2010 was characterized by widespread and intense snowfall. A very dry period followed until mid-February 2011. From then on, snow depths were around 50% of the long-term average at high altitudes. Many snow measurement stations registered new minima. The snow cover disappeared early in May 2011 at high altitudes in the North. However, repeated snowfalls in summer 2011 led to the presence of a mostly continuous snow cover in the high mountains until August.

The extraordinary high air temperatures during the first half of April 2011 caused a timely start of the snow melt, which was the earliest at nearly all PERMOS sites (Figure 2.3). At nearly all locations this was the earliest melt-out observed (in May or in the first half of June) since the beginning of the measurements.

Summer temperatures were above average all over the Swiss Alps (Figures 2.4 and 2.5a). The temperatures reached 25 °C for the first time in the year on 7. April 2011 in Western and Southern Switzerland. The 2nd warmest April (4.6 °C above average 1961–1990) and the 3rd warmest May since 1864 were recorded. From end of June

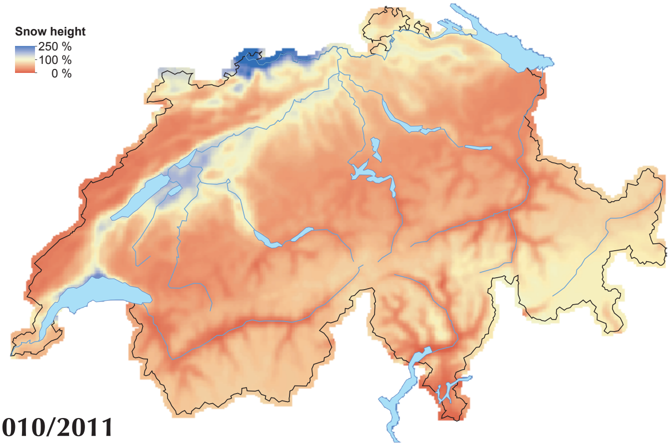

2010/2011

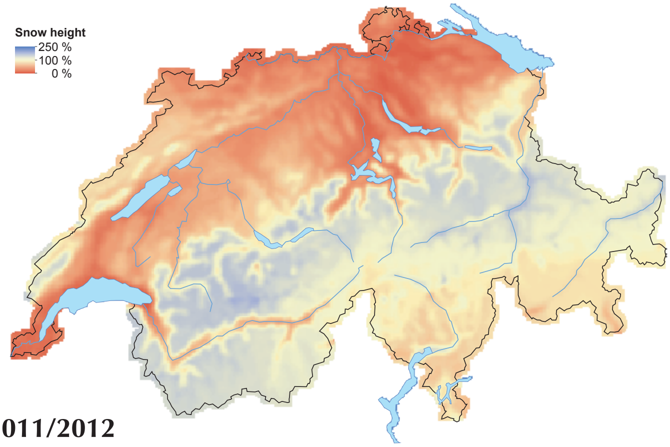

2011/2012

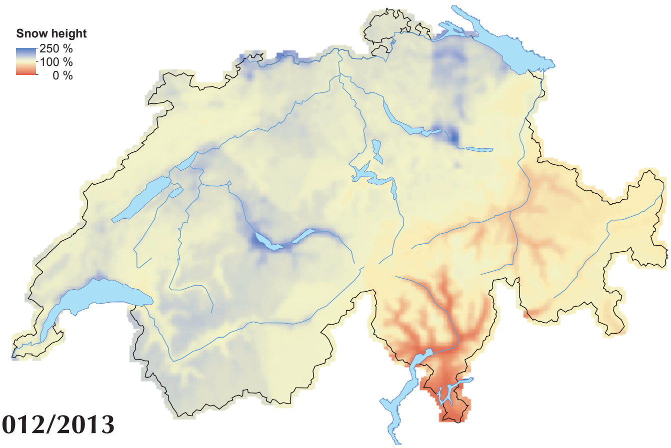

2012/2013

Figure 2.1:
Regional variability of deviations of winter snow amounts for the winters 2010/2011 to 2013/2014 (left page): deviation from the mean value 1971–2000 in percent. Figure provided by C. Marty, SLF.

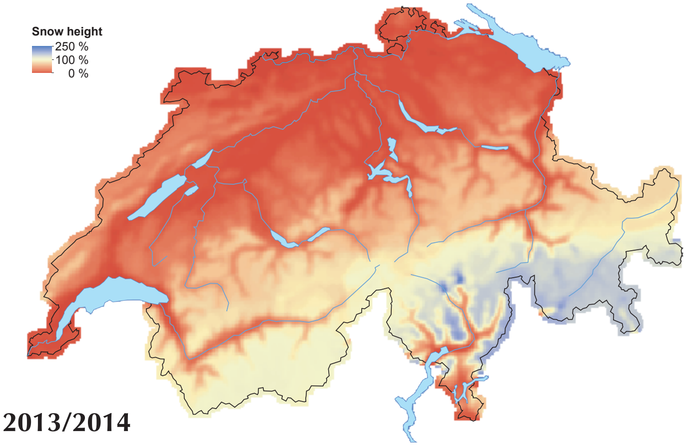

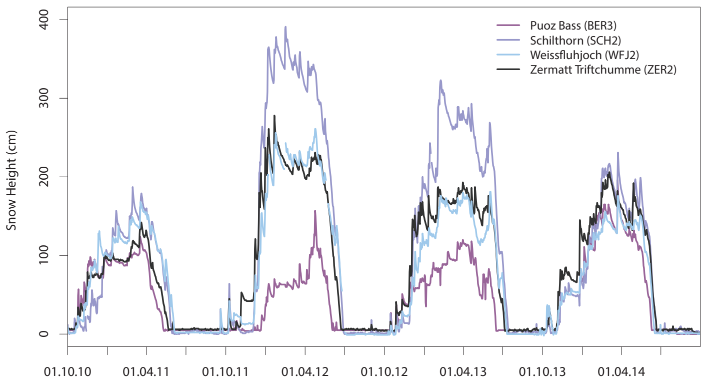

Figure 2.2: Evolution of the snow depth at four measurement stations in the Swiss Alps during the winters 2010/11–2013/14. Data provided by SLF.

until mid-August 2011 it was comparatively cold with lots of thunderstorms. From August until mid-September 2011 warm conditions were observed.

2.2 Air Temperatures and Snow Cover in 2011/2012

The hydrological year 2011/2012 started with a warmer than average autumn (2 °C above average 1961–1990) with high temperatures especially in November 2011. This was followed by extreme cold periods in February 2012, a warm spring (2nd warmest temperatures in March 2012 since 1864), wet weather in the beginning of

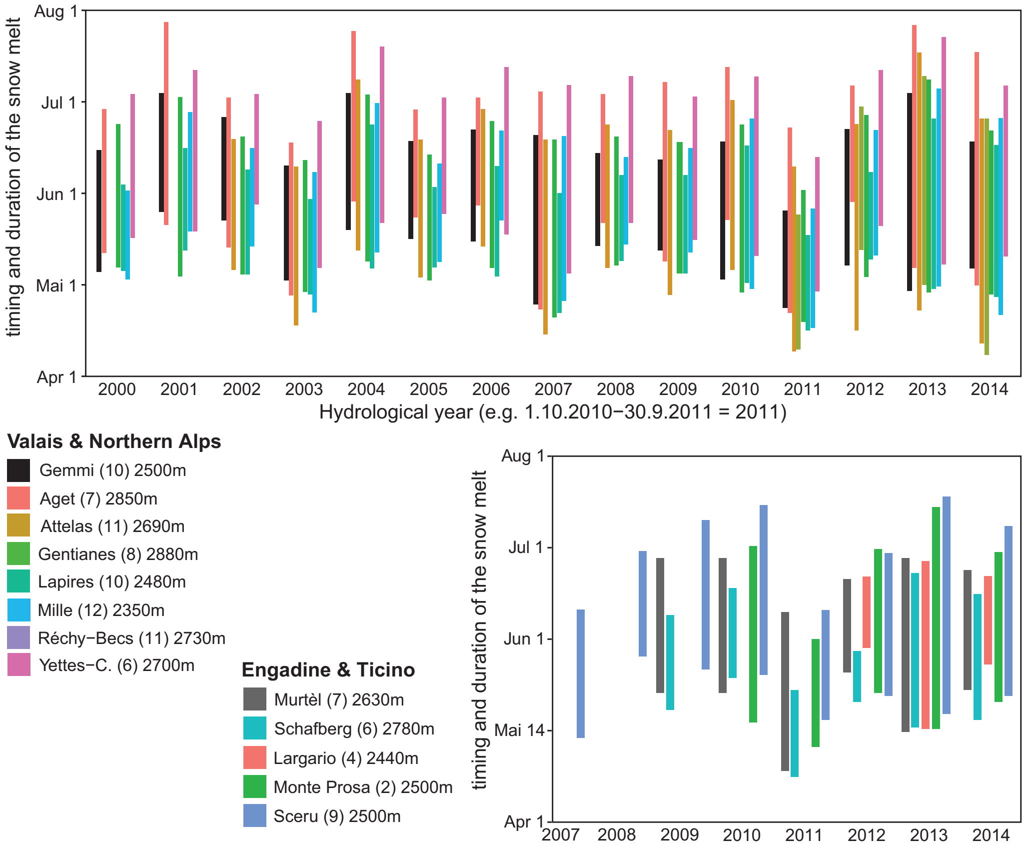

Figure 2.3: *Dates of snow melt (2000–2014) deduced from GST time series. The top and the bottom of the coloured bars indicate the start and the end of the zero curtain period. If several GST-series are measured on a site, the mean is calculated. Legend: site–(number of measurements)–mean elevation.*

summer and high temperatures in August. The year 2012 was on average 1.3 °C warmer than the average from 1961–1990.

Winter 2011/2012 was snow-rich in most regions apart from the upper Engadine and the southern flank of the Alps, where snow depths were below-average (Figures 2.1 and 2.2). Autumn 2011 was very warm and there was only snow at high elevations in the South. In the other regions, the first snowfalls occurred in December 2011. These were intense and continued in January 2012, causing record snow depths on the northern flank of the Alps. Snowfalls continued in April 2012 and snow depths were still above-average in spring. Despite a few snowfalls in summer, all snow was gone by August due to high air temperatures and frequent rainfall.

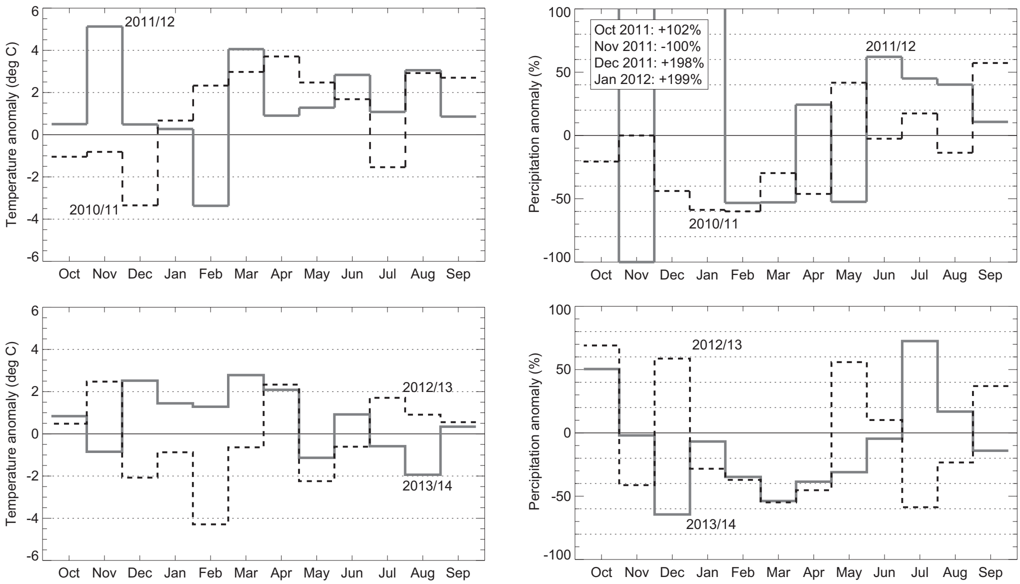

Figure 2.4: *Mean monthly anomalies of air temperatures (left) and precipitation (right) from the long-term climatic mean (period 1981–2010) for the climate station at Weissfluhjoch and the reporting period. Data source: MeteoSwiss, figure compiled by M. Huss, UniFR.*

Despite the low snow amounts at most of the PERMOS sites, the duration of the melting period as well as the melt-out day were more or less equal to the mean of the time series (Figures 2.3 and 2.6). At high elevations the snow cover melted out in June and July.

Summer temperatures were above average in all areas of the Swiss Alps, especially in Valais and Graubünden (Figures 2.4 and 2.5a). Cold and unsettled weather from May until the third week of July 2012 was followed by higher temperatures and heat waves in August. By the end of August and beginning of September an abrupt temperature drop occurred.

2.3 Air Temperatures and Snow Cover in 2012/2013

The beginning of the hydrological year 2012/2013 was characterized by high temperatures in the second half of October 2012, a cold winter in high mountain areas and a warm and sunny summer. Mean annual air temperatures in 2013 were around the average for the new climate norm period 1981–2010. This corresponds to ca. 0.8 °C above average for the former reference period 1961–1990.

Winter 2012/2013 was characterized by above-average snow depths on the northern flank of the Alps and in Valais, average snow depths in most parts of Graubünden, and lower than average snow depths in the upper

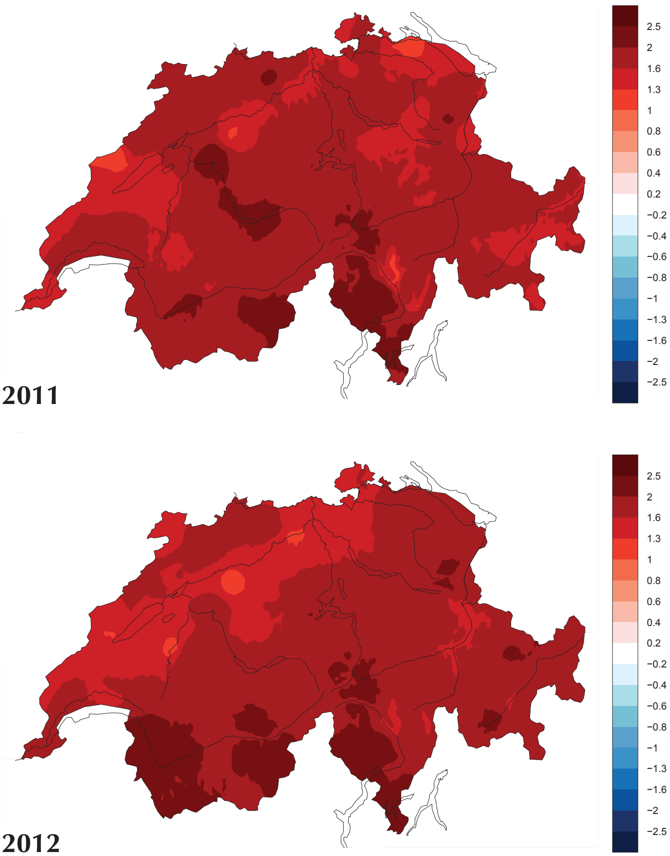

Figure 2.5a:
Regional variability of mean summer air temperatures (May–September) for the summer 2011 (top) and 2012 (bottom), deviation from the mean value 1961–1990 in degrees Celsius. Figure provided by MeteoSwiss.

Engadine and the South of the Alps (Figures 2.1 and 2.2). First snowfalls occurred in October 2012 and were followed by intense precipitation from end of November to mid-December 2012 in the North and the West. Snow depths were two to three times higher than the long-term average. Strong and frequent snowfalls continued until mid-February 2013 in the North. Snow melt usually starts in May, but strong snowfalls from mid-May 2013 until the end of the month caused an important increase in snow depth, particularly on the main ridge of the Alps. In summer 2013, there were only a couple of snowfalls in June and August 2013 at high elevations.

A warm period in April 2013 caused first melt water percolation through the snow cover. Warm and sunny weather during June 2013 caused an intense snow melt. GST measurements (Figure 2.3) show that the duration of the snow melt season was much longer (up to twice as long compared to 2005) and the melt-out was delayed in comparison to the average of the past years.

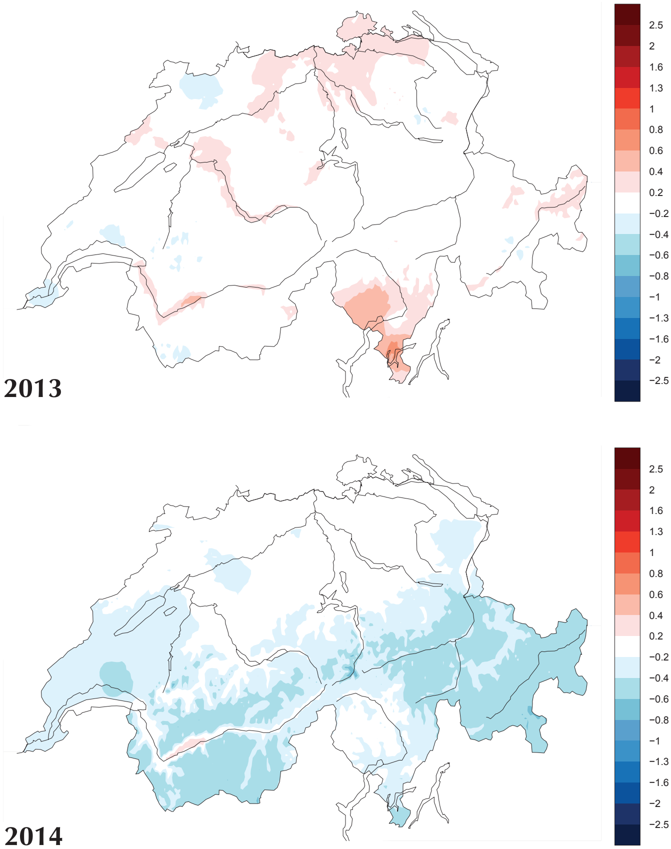

Figure 2.5b:
Regional variability of mean summer air temperatures (May–September) for the summer 2013 (top) and 2014 (bottom), deviation from the mean value 1981–2010 in degrees Celsius. Figure provided by MeteoSwiss.

Summer temperatures in 2013 were around average all over the Swiss Alps (Figures 2.4 and 2.5b). May and June 2013 were dominated by heavy precipitation events and floods, which were interrupted by a short heat wave in June. From July to mid-September 2013 the meteorological conditions were warm and sunny with above average temperatures in July 2013 compared to 1981–2010.

2.4 Air Temperatures and Snow Cover in 2013/2014

The hydrological year 2013/2014 was characterized by many extremes: a very warm autumn with the fourth warmest October, record snow amounts in the South, the third warmest winter, a very warm spring that was followed by a cool and markedly wet midsummer, and eventually the second warmest autumn since measurements started. The mean annual air temperatures in 2014 were 1.24 °C above the average of the climate norm period 1981–2010. The year 2014 was slightly warmer than the previous record year 2011.

Winter 2013/2014 was the third warmest since the beginning of the measurements 150 years ago. It was characterized by lower than average snow depths until Christmas and record high snow depths in the South. Although first snowfalls occurred in October and November 2013, snow depths were only shallow until Christmas due to above average air temperatures. Then, wintery conditions arrived in Switzerland, which lasted until March 2014. Especially the southern flank of the Alps received large snow amounts. Here, snow depth was around twice as high as the average above 1000 m asl. Snow depth was slightly above average in the southern Valais and below average in all other regions (Figures 2.1 and 2.2).

Above average temperatures were measured also in spring 2014 and it was drier and sunnier than usual. Especially March and the first half of April 2014 were mild and sunny, while May was changeable and cool. Snow melt started early in the second half of April, but the snow melt rates in May and June were low, despite of a short heat wave between the 7^{th} and 13^{th} of June (Figure 2.3). The snow disappearance date was close to the long-term average or even slightly above for sites in the South, resulting in rather long snow melt duration. In the northern Alps such as at the Gemmi site, the timing and duration of the snow melt was close to the series mean.

The midsummer months July and August 2014 showed below average temperatures and were markedly wet (Figures 2.4 and 2.5b). The frequent rainy weather lead to the dullest midsummer since measurements started and temperatures were 0.1 to 0.8 °C below the average 1981–2010 for most regions.

Figure 2.6: Snow melt pattern at Blanche de Perroc above the Tsarmine rock glacier site in June 2012. Photo: B. Staub.

3 Ground Temperatures

The basis of the permafrost monitoring is the observation of the subsurface thermal conditions and their changes. Ground temperatures (GT) are measured in 27 boreholes at 16 sites in bedrock and in loose debris on rock glaciers, scree slopes, or moraines (see Table 1.1, Figure 1.4, Table A.1a).

Ground surface temperatures (GST) are measured to characterize the influence of snow and surface cover as well as of topography (slope, aspect, and elevation) on the thermal regime of the ground. The variations of GST mainly reflect short-term variations in atmospheric and snow conditions and their changes are the main driving factor of changes in permafrost conditions at depth. Measurements in the vicinity of the boreholes therefore help to assess the spatial variability at the site and the representativeness of the boreholes. Measurement devices are installed at three main types of locations: (i) in steep bedrock, where the influence of topography on ground temperatures is maximal and a thicker snow or debris cover is absent; (ii) in gently sloping or flat bedrock, where the effect of snow cover becomes important, and (iii) within coarse blocks or debris mantled slopes, where effects of snow cover and air circulation can be observed.

The maximum active layer thickness (ALT) is a reflection of the local snow and atmospheric conditions reigning during the current and previous year, as well as of the local ground characteristics. It is defined by the maximum depth of the 0 °C isotherm in the ground during one year, and is approximated using linear interpolation from thermistors in boreholes.

GT measured at medium depth in boreholes allow the observation of seasonal and inter-annual temperature variations. The temperatures at about 10 m depth do not react to short-term fluctuations but show the seasonal variations and particularly reveal the importance of air temperature and snow depth as regulators of ground temperatures at the regional to national scale. Here, minimum temperatures are typically measured in summer because it takes about six months for a signal at the surface to penetrate. The seasonal signal is hardly visible at ca. 20 m depth (except for steep geometry such as for example the Matterhorn Hörnligrat) and the time lag for signals from the surface is in the order of years. That is, temperature changes at depth are governed by longer-term changes at the surface and trends are reflected delayed but more clearly.

3.1 Near-surface Temperatures

3.1.1 Bedrock

Measurements of near-surface rock temperatures at 10 cm depth at 34 locations within the PERMOS network yielded 23 complete temperature time series of hourly resolution during the hydrological year 2010/2011, 20 during 2011/2012 as well as during 2012/2013, and 17 during 2013/2014. Incomplete data series resulted mostly from broken or lost data loggers. A synopsis of mean annual rock surface temperatures (MARST) is provided in Figure 3.1. The upper part of the illustration shows that MARST are generally higher than mean annual air temperatures (MAAT). In south-exposed near-vertical locations this difference amounts to up to 10 °C, in north-exposed locations MARST is only slightly higher than MAAT. Due to the much larger spread in exposition to solar radiation, the range of relative rock temperatures in steep terrain is about 10 °C whereas it is about 5 °C

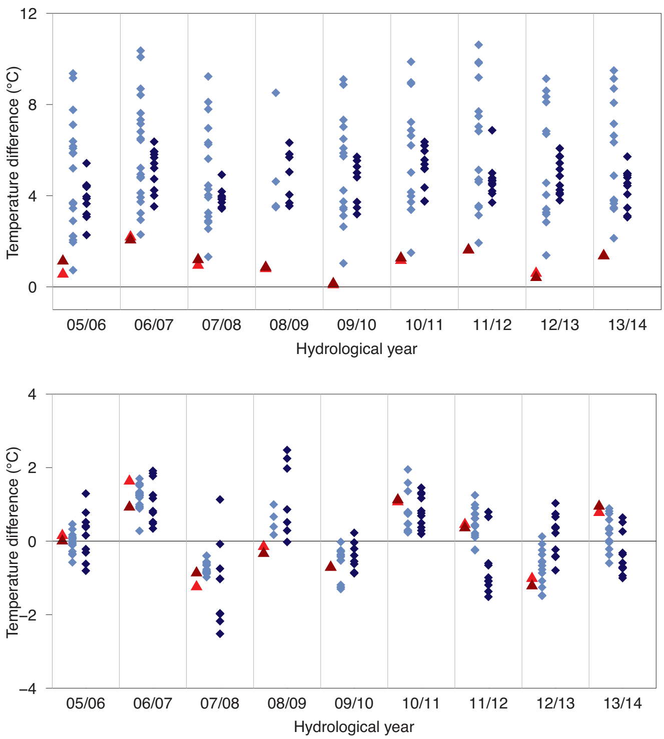

Figure 3.1:
Mean annual rock temperatures plotted for the past nine years: relative to the mean air temperature 1961–1990 (top) and relative to the previous year (bottom). Light blue: steep bedrock without the influence of snow, dark blue: gently inclined rock with seasonal snow cover, darkred: air temperature at Jungfraujoch, red: air temperature at Corvatsch. Mean air temperature was calculated for the elevation of each measurement site based on data from Jungfraujoch and Corvatsch and a constant lapse rate. Air temperature data source: MeteoSwiss.

underneath a seasonal snow cover. The lower part of Figure 3.1 shows that inter-annual fluctuations of temperatures in steep rock correlate more closely with air temperature changes, whereas they exhibit larger variability in rock subject to a seasonal snow cover. MARST in 2010/2011 were around 1 °C higher than during the previous hydrological year. MARST was again slightly higher during 2011/2012 in steep terrain, whereas in less inclined slopes it was lower than in the year before. This is likely a result of the snow rich winter 2011/2012. The opposite pattern can be observed in 2012/2013 when MARST were about 1 °C lower than in the year before in steep rock and only little lower or even higher in flatter bedrock. MARST did not change significantly compared to the previous year in the last year of observation 2013/2014.

3.1.2 Loose Debris

The GST measurements in loose debris material with hourly to 3-hourly resolution were continued at 19 PERMOS sites, which are instrumented with 3–21 single-channel temperature data loggers (Table 3.1). The loggers are typically located on rock glaciers, talus slopes or moraines with slope angles between 0 and 40° around the borehole sites or on rock glaciers where terrestrial geodetic surveys are performed. A relatively thick snow pack typically develops during winter (snow depth from 0.5 to >3 m) at these sites, except for a few that are wind-exposed. A detailed description of the GST sites was published in the appendix of the last report (PERMOS 2013). The parameters derived from these measurements are:

(i) the duration and timing of the snow cover (as described in Chapter 2),
(ii) the Ground Freezing Index (GFI), which is the sum of all daily negative temperatures measured during winter and indicates how cold a winter is at the ground surface (a lower GFI results from a colder winter), and
(iii) the Mean Annual Ground Surface Temperatures (MAGST), which are calculated in the form of 365-day running mean of daily averages and represent inter-annual GST variations.

Table 3.1: GST sites and start of the ground surface temperature measurements. T=temperature site, K=kinematics site, BTS=site with BTS measurements (see Tab. 3.2 and Figure 3.4). Brackets mark data not included in PERMOS, reference sites are marked in bold. On Jungfraujoch only rock surface temperatures are measured.

Site	Region/Valley	Since	T	K	BTS
Aget	Val de Bagnes, VS	1998		x	
Attelas	Val de Bagnes, VS	2001	x		
Alpage de Mille	Val de Bagnes, VS	1997		x	x
Dreveneuse	Chablais, VS	2004	x		
Gemmi-Furggentälti	Berner Oberland, BE	1994		x	
Gentianes	Val de Nendaz, VS	2010	x		
Grosses Gufer	Upper Valais, Aletsch, VS	2012		x	
Jungfraujoch	Berner Oberland, BE	2001	x		
Lapires	Val de Nendaz, VS	1998	x	x	x
Monte Prosa	Gotthard, TI	2009		x	
Murtèl-Corvatsch	Upper Engadine, GR	2000	x	x	
Réchy	Val de Réchy, VS	1997		x	(x)
Schafberg	Upper Engadine, GR	2000	x		
Schilthorn	Bernese Oberland, BE	1999	x		
Stabbio di Largario	Valle di Blenio, TI	2009		x	
Tsarmine	Val d'Arolla, VS	2007		x	
Tsaté	Val d'Hérens, VS	2009	x		
Turtmanntal-Hungerlitälli	Upper Valais, VS	2010		x	
Valle di Sceru	Valle di Blenio, TI	2006		x	
Yettes Condjà	Val de Nendaz, VS	1998		x	

For this report, major efforts have been undertaken to fill gaps in the GST data and to estimate the uncertainty resulting on aggregates and indices (Staub et al. 2016). As a result, the analysis for PERMOS are now being done on the basis of daily means with automated processing routines directly applied on the PERMOS data base.

Ground Freezing and Thawing Indices

In 2010/2011 and 2011/2012 the Ground Freezing Index (GFI) was slightly lower than during the three preceding years but clearly higher than in 2005/2006 and 2006/2007, especially in the Valais (Figure 3.2). The ground freezing was low at all of the observed sites in 2012/2013 and in 2013/2014 due to the early onset of the snow cover and high snow depths.

Regarding the Thawing Index (THI, sum of all daily positive temperatures measured between the snow melt and the end of the hydrological year), inter-annual variations are smaller compared to the GFI. THI was slightly higher during the reporting period (i.e. warmer conditions) than in the preceding years, but still remained below the maxima observed in summer 2003. The warmest summer of the reporting period was 2011, because of the early melt-out and the high air temperatures in August and September 2011 (see Chapter 2.1). Minimal THI values were measured in 2014 due to the rainy weather during summer (see Chapter 2.4).

Mean Annual Ground Surface Temperature

The MAGST values illustrated in Figure 3.3 are calculated using running 365-day averages of daily means (aggregated at the end of the period). MAGST remain at a comparably high level from 2009 onwards with smaller inter-annual variations than between 2001 and 2008. However, the maxima observed in 2003 (superposition of the strongly limited ground cooling in winter 2002/03 and the summer heat wave 2003) have not yet been reached. The majority of the MAGST curves are highly similar in terms of relative changes over time when comparing mean time series (representative for single sites): Regional differences are rather small and either related to different snow regimes (e.g., north and south exposition at the Schilthorn) or to site-specific processes (e.g., ventilated parts of talus slopes as observed at Dreveneuse or Lapires).

3.1.3 BTS

BTS mapping is performed within PERMOS to provide a snapshot on the thermal state of the ground in the second part of the winter season (typically in March). The ground surface temperature is assumed to be relatively stable at this time of the year and to reflect the intensity of the cooling from the surface during winter. A complete series of yearly BTS and snow depth measurements is available for Alpage de Mille with measurements undertaken from 1996 onwards. A less complete series from Lapires is used for comparison (Table 3.2, Figure 3.4). Mean values of winter BTS temperatures in 2011 were slightly below average and snow depths were comparably small. Mean BTS values were again nearly average in 2012. Snow depths were below average at Alpage de Mille and much smaller than at Lapires, where they were above average as it occurred already in 2008. BTS values as well as snow depths were higher in 2013 with snow conditions similar to those in 2009. The second

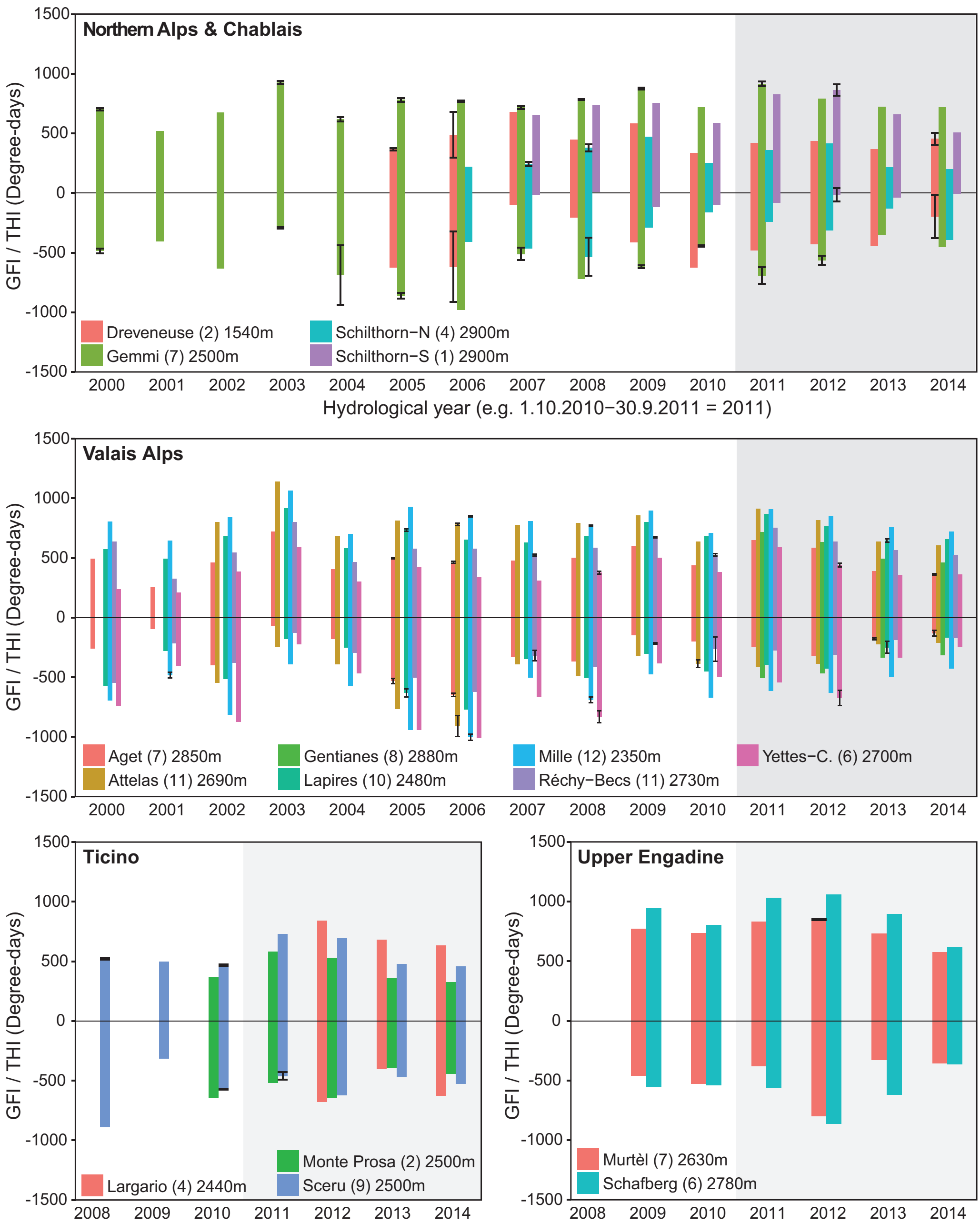

Figure 3.2: Ground freezing and thawing index (GFI/THI) at GST sites: a) Northern Alps and Chablais, b) Valais, c) Ticino and d) Engadine. The error bars illustrate estimated uncertainty resulting from the filling of data gaps. Legend: site-(total number of sensors)-mean elevation.

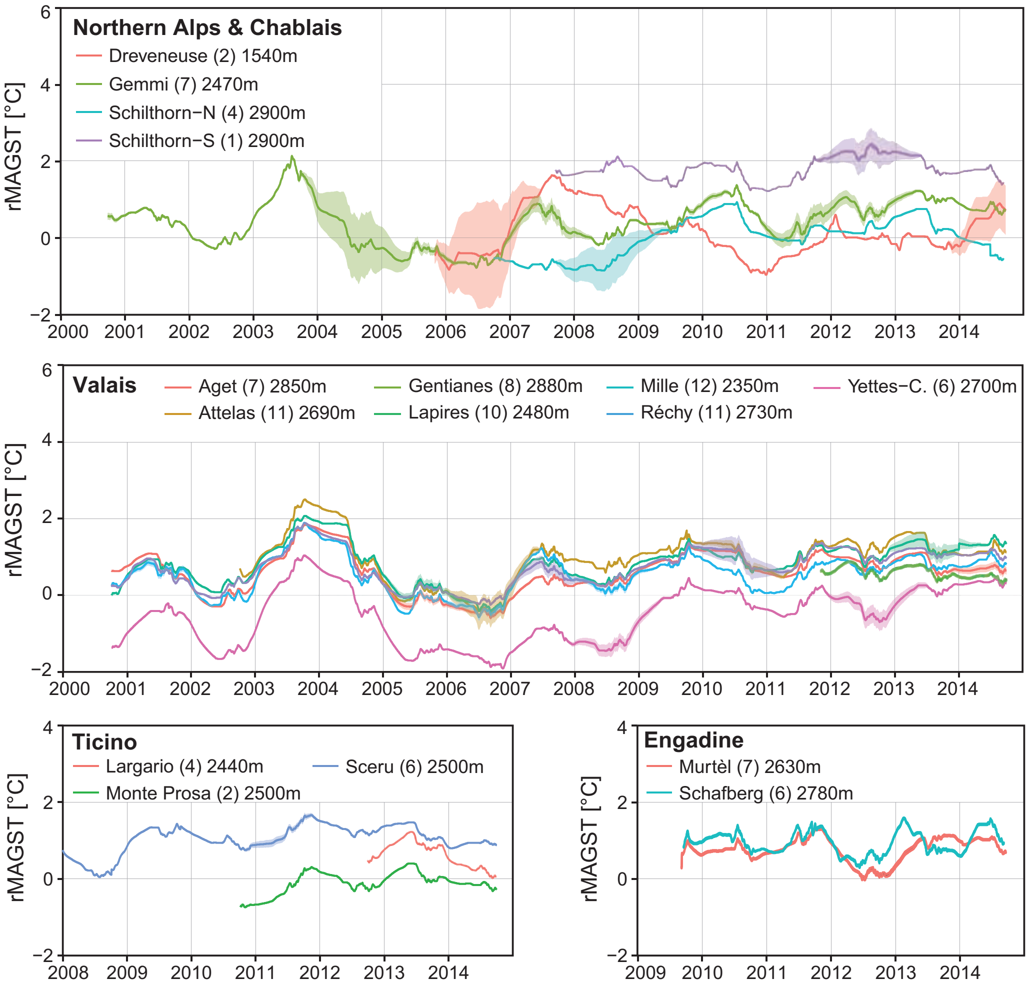

Figure 3.3: *Evolution of the mean annual ground surface temperature (MAGST): a) Bernese Oberland, b) Lower Valais, c) Engadine. MAGST is computed as running annual mean based on monthly aggregation and plotted at the end of the averaging period. The shaded areas illustrate the estimated uncertainty range resulting from gap filling. Legend: site-(total number of sensors)-mean elevation.*

highest BTS temperatures since 1996 (maximum in 1997) were measured in 2014 at Alpage de Mille with snow depths close to the long-term average.

In summary, the long BTS-monitoring series from Alpage de Mille and Lapires show that single and unrepeated BTS campaigns are not representative for a specific point or area, because BTS are highly influenced by the snow conditions during and before the surveys. BTS measurements are, however, very valuable to get spatial information on the thermal conditions and the winter cooling over a specifc area. They illustrate the considerable inter-annual GST variations in wintertime which are strongly related to the snow cover duration.

Table 3.2: Date of BTS measurements 2011–2014.

Site	Region	Available BTS	BTS 2011	BTS 2012	BTS 2013	BTS 2014
Alpage de Mille	Val de Bagnes, VS	since 1996	07.03	07.03	04.03	13.03.
Lapires	Val de Nendaz, VS	since 2001	14.03	09.03.	n.a.	26.02.

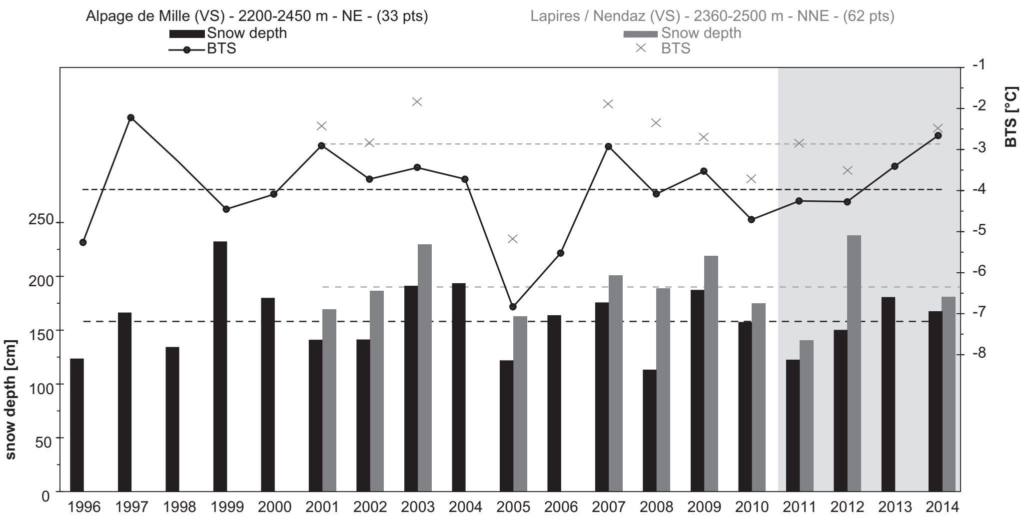

Figure 3.4: Mean BTS and snow depth since 1996 on two sites in the Lower Valais. Dotted lines are the mean values for available BTS and snow depth time series at Alpage de Mille (1996–2014, black) and Lapires (2001–2014, grey).

3.2 Borehole Measurements

The PERMOS network includes 27 boreholes at 16 sites (see Figure 1.1 and Table A.1).

3.2.1 Active Layer Thickness

The maximum active layer thickness (ALT) for the years 2011–2014 was determined for most of the 27 boreholes. It could not be determined for some boreholes because they have data gaps or drifting sensors (MBP_0196, MBP_0296, MUR_0299), they are not located in permafrost (GEM_0106, MUR_0199) or do not reach the surface (JFJ_0195). Maximum ALT and the corresponding date are given in Table 3.3, and in Figure 3.5 for selected boreholes. A complete list of the ALT for all years and boreholes is provided in the Table A.2.

ALT remained more or less constant during the reporting period in several boreholes with an ice-rich subsurface: ATT_0108, COR_0200, FLU_0102, LAP_0198, MUR_0499, SBE_0290. A number boreholes registered ongoing and gradual active layer deepening, such as COR_0287, GEN_0102, LAP_1108, LAP_1208 and STO_6100. The ALT in borehole COR_0287 reached more than 4 metres depth for the first time in 2012, after nearly constant 23 years between 1988 and 2010. The largest increase in ALT during the observation period was observed in the ice-rich moraine in Gentianes (GEN_0102). Here, ALT increased from 2 to >4 metres. Although no borehole registered ALT thinning over the entire period, a reduction in ALT of 0.5 m was registered in RIT_0105 between 2010 and 2011 and other boreholes registered fluctuations of several centimetres from year to year. The active layer for SCH_5198 reached down to nearly 7 metres since 2009, but was considerable less deep in summer 2014 (Figures 3.5 and 3.7).

3.2.2 Borehole Temperatures

Temperatures measured in the boreholes during the reporting period are depicted in Figure 3.6, detailed figures with ground temperatures for all boreholes of the network are included in the Appendix (Figures A.1–A.26).

The observed warming trend during the previous reporting period 2008–2010 continued after 2010 in most of the boreholes. The generally above average warm weather conditions, the exceptionally warm summers in 2011 and 2012 as well as the record warm year 2014 (see Chapter 2) led to an overall rising trend in ground temperature at the observed sites in the Swiss Alps. This is especially true for the maxima, which are measured in winter at 10 m depth and reflect summer conditions. In contrast, the minima are influenced by local snow conditions in winter. For example, the boreholes located in the Engadine registered lower minima in winter 2012/2013 than in the previous four winters, due to the lack of snow. A general rising trend in borehole temperatures since 2009 can also be observed at 20 m depth. This trend is more pronounced in colder locations than in locations with temperatures close to 0 °C due to the effect of latent heat. For most boreholes and depths the permafrost conditions are warmer than in the record year 2003 at the end of the reporting period.

Table 3.3: Maximum active layer thickness (ALT) measured in the boreholes in metres.

Name	2011		2012		2013		2014	
	ALT	Date	ALT	Date	ALT	Date	ALT	Date
Attelas 0108	3.9	08.09	3.9	25.08	3.9	08.09	3.9	16.10
Attelas 0208	5.0	20.08	5.0	15.08	5.4	29.09	5.0	08.09
Corvatsch 0200	2.5	06.09	2.4	24.08	2.5	09.09	2.5	11.10
Corvatsch 0287	3.8	06.10	4.1	06.10	4.2	25.09	4.2	02.09
Flüela 0102	3.0	17.09	3.0	24.08	3.0	07.09	3.0	29.08
Gentianes 0102	3.1	20.10	3.0	08.10	4.0	12.12	4.4	17.12
Lapires 0198	5.2	24.09	5.2	11.10	5.2	26.10	5.2	13.10
Lapires 1108	4.6	08.10	4.8	08.10	5.3	21.11	–	–
Lapires 1208	4.6	08.10	4.5	24.09	4.6	09.10	4.7	19.09
Matterhorn 0205	3.6	20.09	3.4	15.09	3.4	10.09	2.7	13.09
Muot da B. P. 0196	–	–	–	–	–	–	–	–
Muot da B. P. 0296	–	–	–	–	–	–	–	–
Muragl 0499	4.6	18.08	4.6	19.08	4.5	22.06	–	–
Ritigraben 0105	3.4	16.09	3.5	15.09	–	–	3.2	23.09
Schafberg 0190	–	–	–	–	–	–	–	–
Schafberg 0290	5.2	22.09	5.1	30.08	5.1	10.09	5.1	21.08
Schilthorn 5000	6.8	28.09	6.8	08.09	6.9	26.10	8.9	18.10
Schilthorn 5198	6.7	10.10	6.9	26.11	7.7	17.11	4.9	19.10
Schilthorn 5200	2.9	27.09	3.3	10.10	3.2	26.10	2.9	20.10
Stockhorn 6000	4.0	10.10	3.7	26.09	3.5	16.09	3.3	13.10
Stockhorn 6100	4.6	03.12	4.7	08.12	4.8	14.12	4.8	06.12
Tsaté 0104	6.9	21.11	7.7	16.09	7.7	18.09	7.3	18.10

3.3 Summary

GST measurements reflect atmospheric conditions and the duration and thickness of the snow cover. They are high since 2009 even though GFIs of 2010/2011 and 2011/2012 were lower than in the three preceding years. In general, mean annual ground surface temperatures were higher than during the previous reporting period but they did not reach the maxima from 2003.

ALTs increased for most borehole sites during the reporting period, but remained more or less constant for some boreholes. The ground temperatures show a warming trend that has started in the year 2009 and continued during the four years of observation. Ground thermal conditions are generally warmer than in the hot year 2003 at the end of the reporting period.

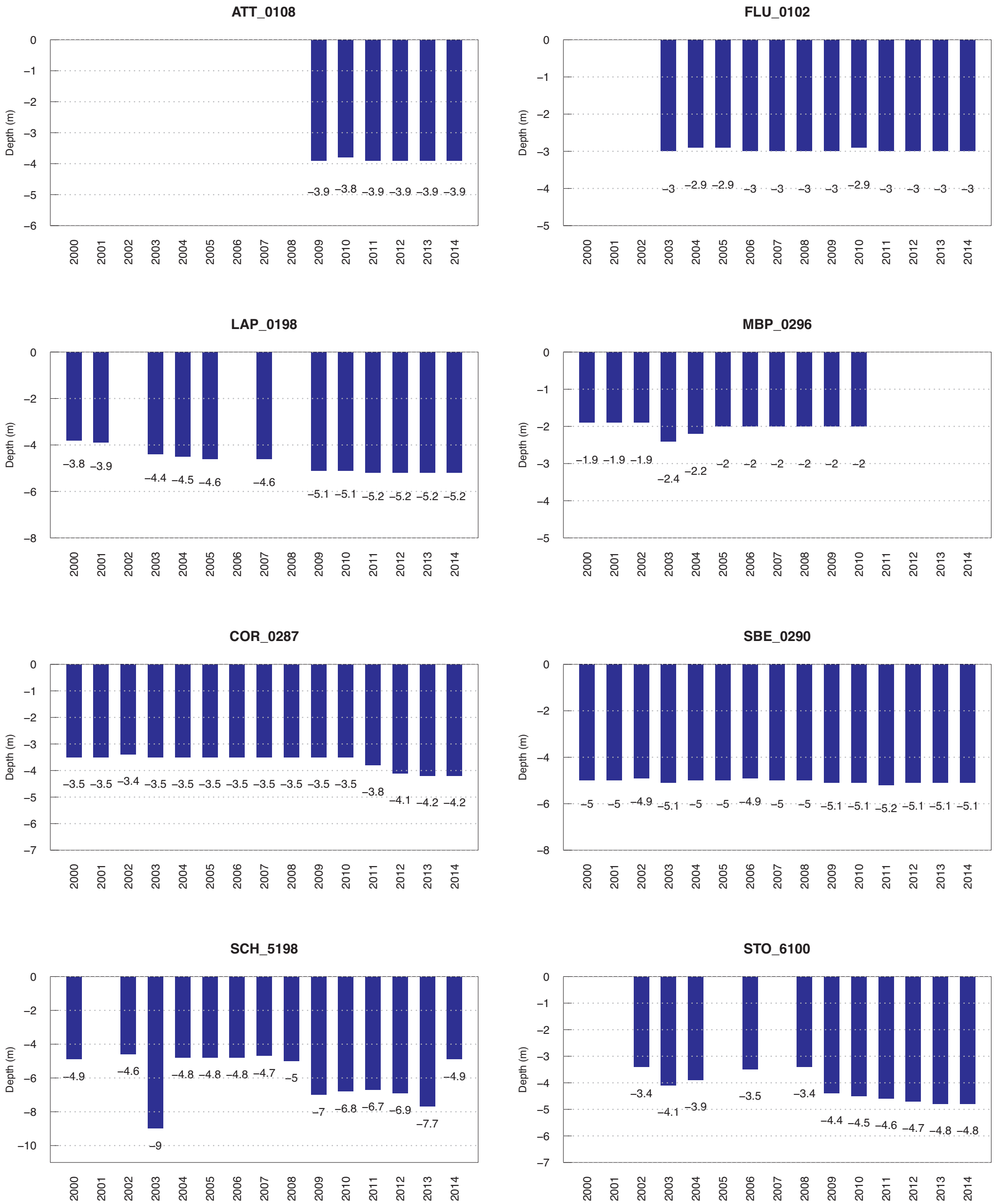

Figure 3.5: *Maximum active layer thickness measured at selected reference sites in the past 15 years: Les Attelas (ATT_0108), Flüela (FLU_0102), Lapires (LAP_0198), Muot da Barba Peider (MBP_0296), Corvatsch-Murtèl (COR_0287), Schafberg (SBE_0290), Schilthorn (SCH_5198), Stockhorn (STO_6100).*

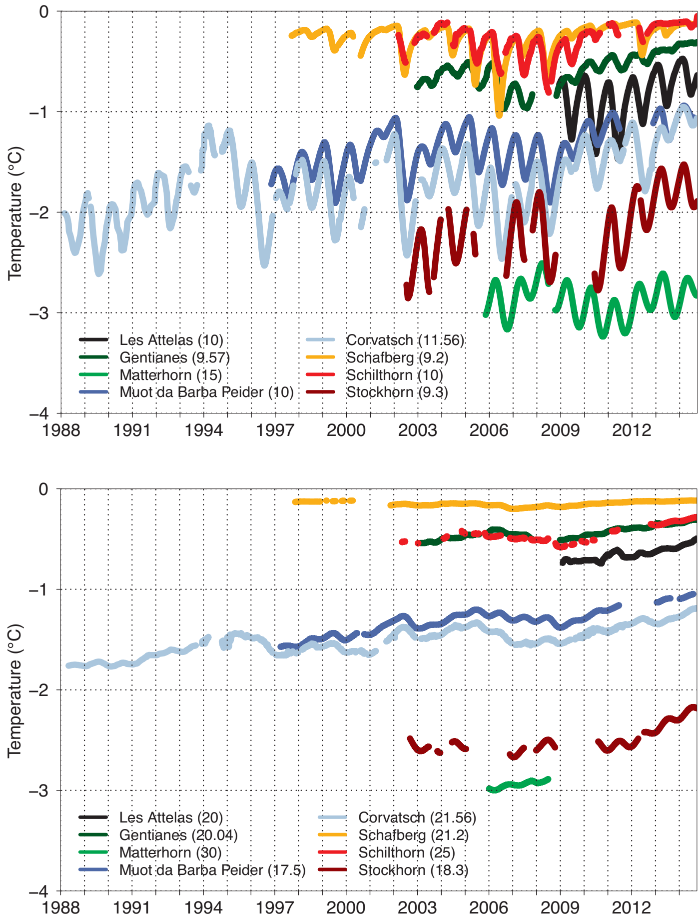

Figure 3.6: Daily ground temperatures measured in selected boreholes at ca. 10 m and ca. 20 m depth. For each borehole, the data measured at the thermistors closest to 10 m and 20 m depth is plotted. The exact depth in metres is indicated in brackets in the legend.

Figure 3.7: Borehole site at the Schilthorn, Bernese Oberland. The covers for borehole SCH_5200 (right) and SCH_5000 (centre, flat) can be seen in the foreground, the energy balance and borehole measurement station and the smaller mast of the automatic ERT are seen in the back. The borehole station was renovated in summer 2011. Photo: J. Nötzli, August 2011.

4 Electrical Resistivities

The measurement of the two-dimensional distribution of electrical resistivities in the ground were continued for six permanent profiles at four sites, including a rock glacier, a talus slope, and two bedrock sites (Table 4.1). All profiles are located close to boreholes to characterise the location and allow for a joint analysis of the borehole temperatures with the temporal changes in resistivities, which are indicative for changes in water and ice contents. The electrical resistivity tomography (ERT) monitoring of the Flüela Pass profile could not be continued after 2011 because of severe rock fall from the cliffs above the Schottensee onto the talus slope where the borehole is located.

4.1 ERT Results for 2010 to 2014

Figures 4.1 and 4.3–4.5 (upper panels) show tomograms for all sites and compare the ERT results of measurements from August/September of consecutive years. The inter-annual changes in resistivities (in %) indicate changes in the ice and unfrozen water content and are shown in the lower panels. Red colours highlight a decrease in resistivities with time and basically point to an increase in unfrozen water content and/or a decrease in ice content. A resistivity increase (blue colours) may be caused by ice aggradation and/or drained pore water.

A significant decrease of electrical resistivities was observed at Schilthorn in the entire profile in 2009 and 2010, which persisted at this record low since then. Figure 4.2 shows that in 2009 the average resistivities fell for the first time even below the values of summer 2003, and they stayed at this low level since then. In comparison, the borehole temperatures were well below values from summer of 2003 although they were rather high. These very low resistivity values indicate a strong decrease in the average ice content to the lowest level since the beginning of the ERT monitoring in 1999 (see Figure 4.2).

Table 4.1: Overview of all ERT monitoring sites and profiles. «# electr.» denotes the number or electrodes, «length» the length of the profile, «app-d» the approximate depth of investigation and «BH-dist horiz.» is the horizontal distance to the borehole(s).

ERT-Site	Location	# electr./ spacing (m)	length/ app-d (m)	BH–dist horiz. (m)	ERT since
Schilthorn (SCH)	horizontal profile in N-slope	30/2	58/10	51/98: 11	Aug 99
				50/00: 26	
Schilthorn (SCV)	vertical profile across crest (N-S)	47/4	184/30	51/98: 20	Aug 06
Corvatsch-Murtèl (MT)	longitudinal along rock glacier	48/5	235/40	02/87: 55	Aug 05
Stockhorn (ST)	N-S-profile across plateau	55/2	108/15	60/00: 28	
				61/00: 57	Sep 05
Lapires (LAH)	horizontal profile in N-slope	43/4	168/25	01/98: 112	Aug 06
Lapires (LAV)	vertical profile in N-slope	70/4	276/25	01/98: 108	
				12/08: 188	
				13/08: 264	Jun 07

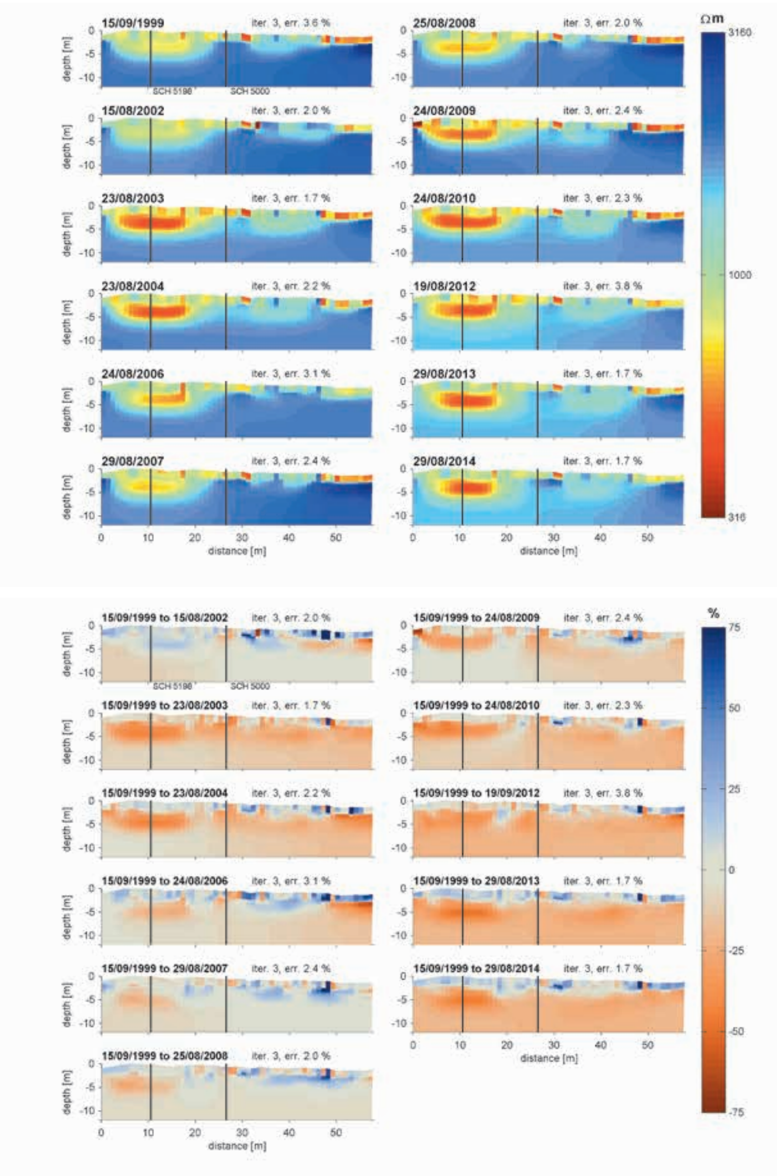

Figure 4.1: *Tomograms showing the resistivity distribution (top) and the temporal resistivity change (bottom) for the years 1999–2013 of the horizontal ERT profile in the northern slope of the Schilthorn crest.*

At the Stockhorn site (cf. Figure 4.6), a consistent long-term comparison of the annual measurements is only possible for the years 2012 and 2013 because the measurement dates are comparable with the date of the first measurement in September 2005 (no measurements are available in 2009 and 2011). The borehole temperatures in 2012 and 2013 have been among the warmest since the beginning of the measurements like for many other sites (cf. Figure 3.6) and accordingly, resistivities are relatively low in the uppermost 10 m of the ground (Figure 4.3). The resistivity decrease during the last years is especially pronounced near the borehole STO_6100 and in the southern part of the plateau in agreement with the borehole temperatures. Almost no changes are observed around borehole STO_6000 and in the northern part of the plateau.

The resistivity changes between 2005 and 2010 rather reflect seasonal signals (e.g., thawing of the active layer or the advance of the warming front in summer), than annual changes of the permafrost conditions, as the measurement dates vary between beginning of August to end of September.

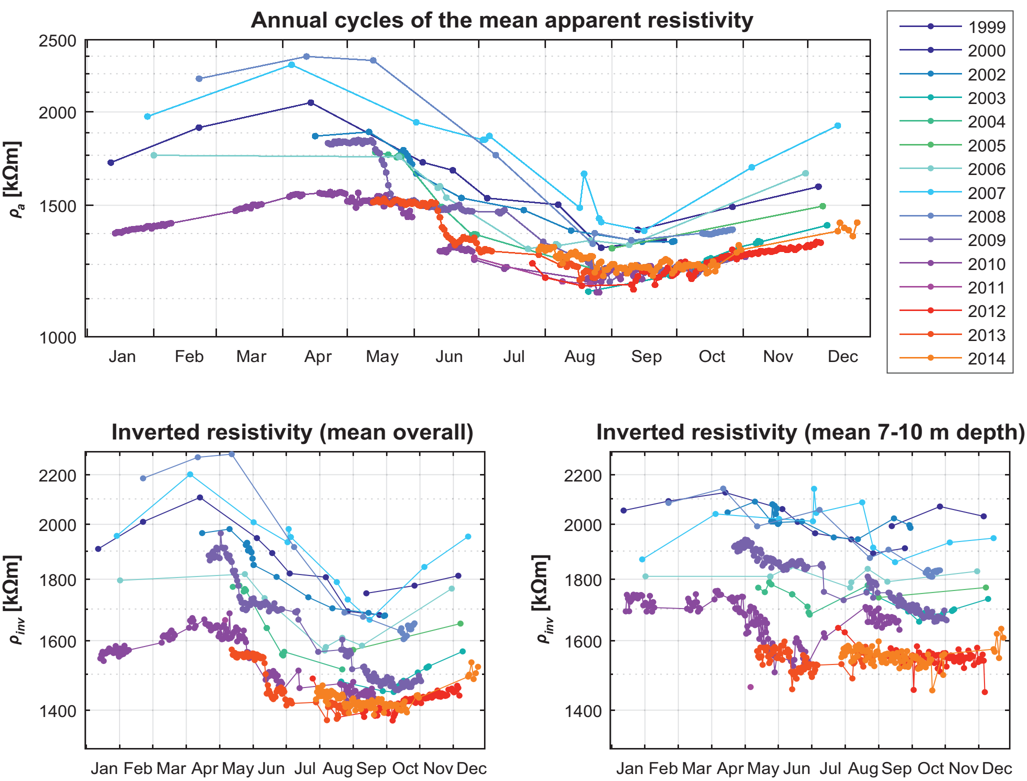

Figure 4.2: Annual cycles of average apparent (top) and inverted (bottom) resistivities per measurement since 1999 for the horizontal ERT profile in the northern slope of the Schilthorn (SCH). To illustrate better inter-annual resitivity changes, the last panel focuses at the permafrost table (7–10 m depth). Figure compiled by C. Mollaret, UniFR.

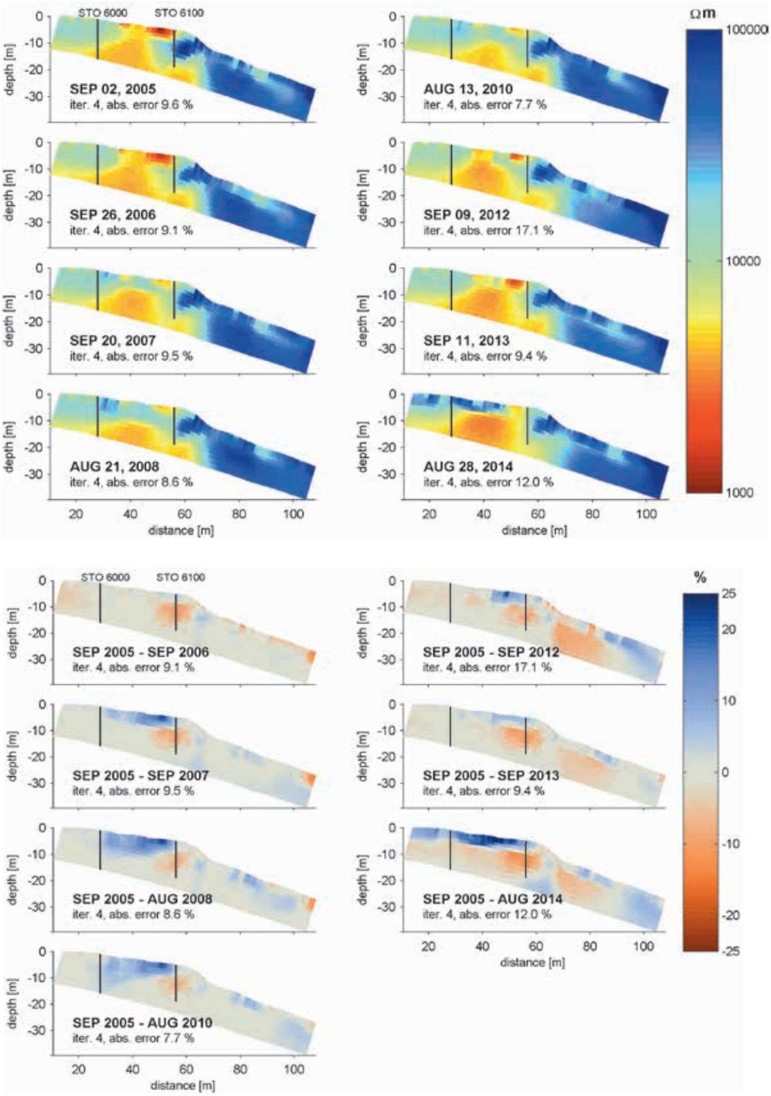

Figure 4.3: *Tomograms showing the resistivity distribution (top) and the temporal resistivity change (bottom) for the years 2005 to 2014 of the ERT profile across the Stockhorn plateau (ST).*

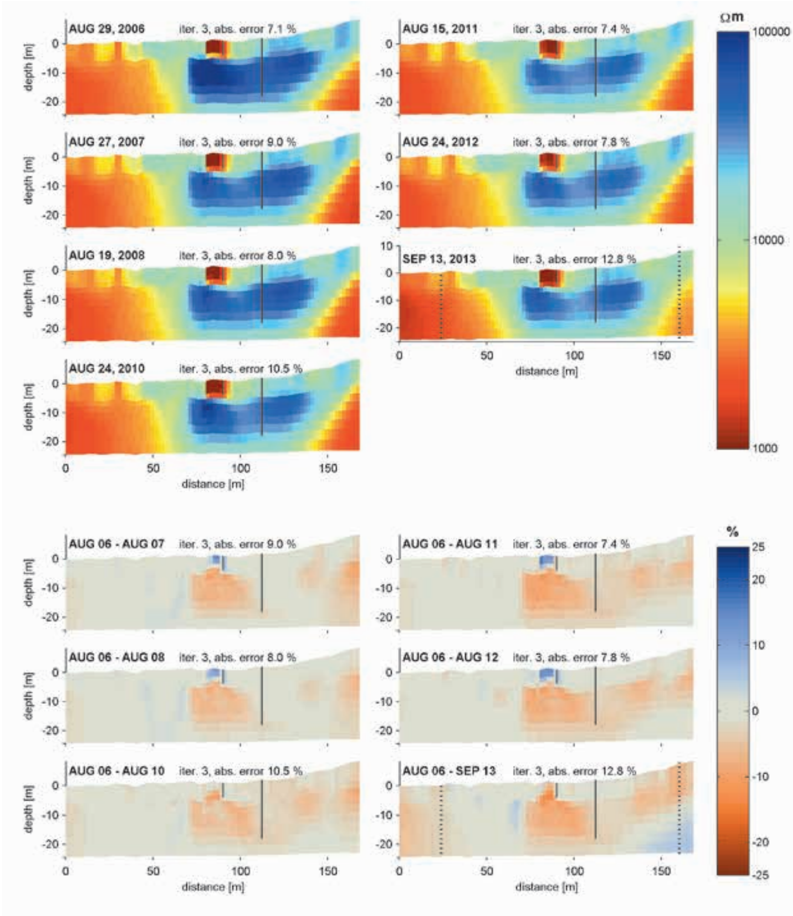

Figure 4.4: *Tomograms showing the resistivity distribution (top) and the temporal resistivity change (bottom) for the years 2006 to 2013 of the horizontal ERT profile in the Lapires talus slope (LAH).*

A marked and persisting resistivity decrease can also be observed at the Lapires talus slope since 2010 within the permafrost body (indicated by the blue zone in the upper panels of Figure 4.4). Again, this change is consistent with the observed borehole temperatures, which indicate increased active layer depths since 2009 (cf. Figure 3.5). The even stronger decrease in resistivities observed in 2013 is, however, rather due to the later measurement date compared to all other measurements, and may reflect the seasonal effect of the advance of the warming front. Interestingly, the resistivity decrease at Lapires is not just observed at the top of permafrost but for the entire profile. Even if the permafrost body is not very thick, this is confirming the important role of the internal air circulation within and below the ice-rich zone for the evolution of the permafrost at this site.

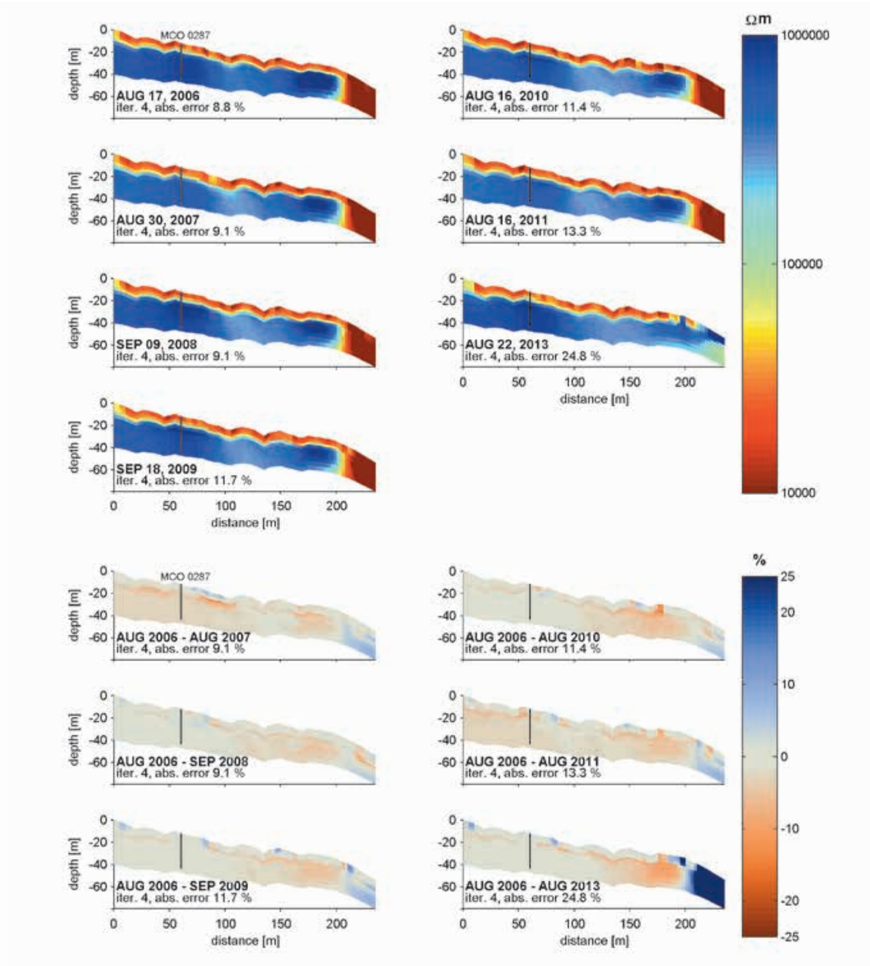

Figure 4.5: Tomograms showing the resistivity distribution (top) and the temporal resistivity change (bottom) for the years 2006 to 2013 of the longitudinal ERT profile across the frontal part of the Murtèl rock glacier (MT).

The Murtèl rock glacier has the highest overall resistivity values in the ERT network because of its very high ice content. Resistivity changes in such resistive material have to be interpreted with great care, and misinterpretation of inversion artefacts due to the strong resistivity contrast between the active layer and the ice body have to be avoided (Hilbich et al. 2009). In general, only resistivity changes in the uppermost few metres are reliable without further evidence. Compared to the resistivity changes in previous years, a slight decreasing tendency in resistivities can be observed at the top of the permafrost in the frontal part of the rock glacier (between 100 and 200 m distance) since 2010 (Figure 4.5). This may indicate a melting of the ice core from above (or an increased unfrozen water content in the still frozen ice core) in the past years. This would be in agreement with the observed higher borehole temperatures. The data set from 2013 has, however, a low quality around the rock glacier front due to a broken cable, and both, the very high resistivities at the front and the strong resistivity decrease in the ice-rich zone close to the front are likely rather a consequence of this measurement error than a permafrost signal.

4.2 Summary

At all ERT monitoring sites a significant decrease of the measured resistivities was observed in the period 2010–2014. While at most sites these changes are only observed in parts of the profile, the Schilthorn data set shows a considerable resistivity decrease in the complete profile with the lowest values since the start of ERT monitoring in 1999. This is attributed to a cumulative effect of the rather warm years since 2009, which is also visible in the borehole temperatures and the larger than average active layer thicknesses (see Chapter 3.2).

Figure 4.6: Geophysics measurements at the Stockhorn site. Photo: C. Hilbich.

5 Kinematics

Rock glaciers are key landforms in high mountain permafrost and their movements reveal indirect information on the ground thermal conditions within these landforms. The creep behaviour of ice-rich permafrost follows an exponential relation with ground temperature and the largest part of the movement is supposed to happen within one or several shear horizons at 10–30 m depth (Arenson et al. 2002). Continuous long-term data series of permafrost creep are obtained at 14 rock glacier sites of the PERMOS network in order to provide a basis for the understanding and investigation of ongoing processes and dynamics.

5.1 Monitoring Strategy

The kinematic monitoring is based on aerial surveys (AS) and terrestrial geodetic surveys (TGS, by total station or differential GPS). This combination of methods was inclued into PERMOS because significant seasonal, inter-annual and long-term variations in rock glacier kinematics were observed (Delaloye et al. 2010, PERMOS 2013). The aim is to analyse geometry changes (i.e., horizontal velocities and vertical changes) in detail, to quantify permafrost creep and to observe signs for potential permafrost degradation (such as vertical thinning due to ice melt or rock glacier destabilization). On most monitored rock glaciers GST are also measured and on rock glacier Corvatsch-Murtèl ERT monitoring is performed since 2005 (see Chapter 4).

Aerial photographs are taken every 2–5 years (depending on the rock glacier velocity and the flight planning) from low altitudes (scale about 1:6'000) to monitor rock glaciers in different regions of the Swiss Alps since the beginning of PERMOS in 2000. Digital terrain models (DTM's) as well as orthophotos are compiled to describe and quantify horizontal and vertical deformation rates for the entire landform at a multi-annual to decadal scale. Terrain movements can be determined for large areas at high spatial resolution (10–30 cm) and dense flow fields can be derived (see Figure 5.1).

TGS are performed at a number of rock glaciers in the Swiss Alps and were included into the PERMOS monitoring strategy in 2008. They comprise at least one survey per year, always at the same time in the season (usually in late summer) for a number of selected blocks on each rock glacier (10–100 points). Most TGS sites (see Tables 1.1 and 5.1) were established within research projects and observed for several years up to decades. Horizontal (Δxy) and vertical (Δz, ratio of slope) changes are quantified based on coordinates (x, y) and altitude (z) with accuracies of 1–3 cm relative to a common coordinate reference system. The analysis of the data includes studying the temporal evolution of representative sets of points, usually in the central zones of the rock glacier lobes. In addition, trajectories and flow fields can be generated.

A pilot study was launched in 2013 to evaluate the use of permanently installed GPS sensors for long-term permafrost monitoring. These permanent GPS devices increase the temporal resolution of the kinematic monitoring to the seasonal to daily scale for a small number of points (see for example Wirz et al. 2015).

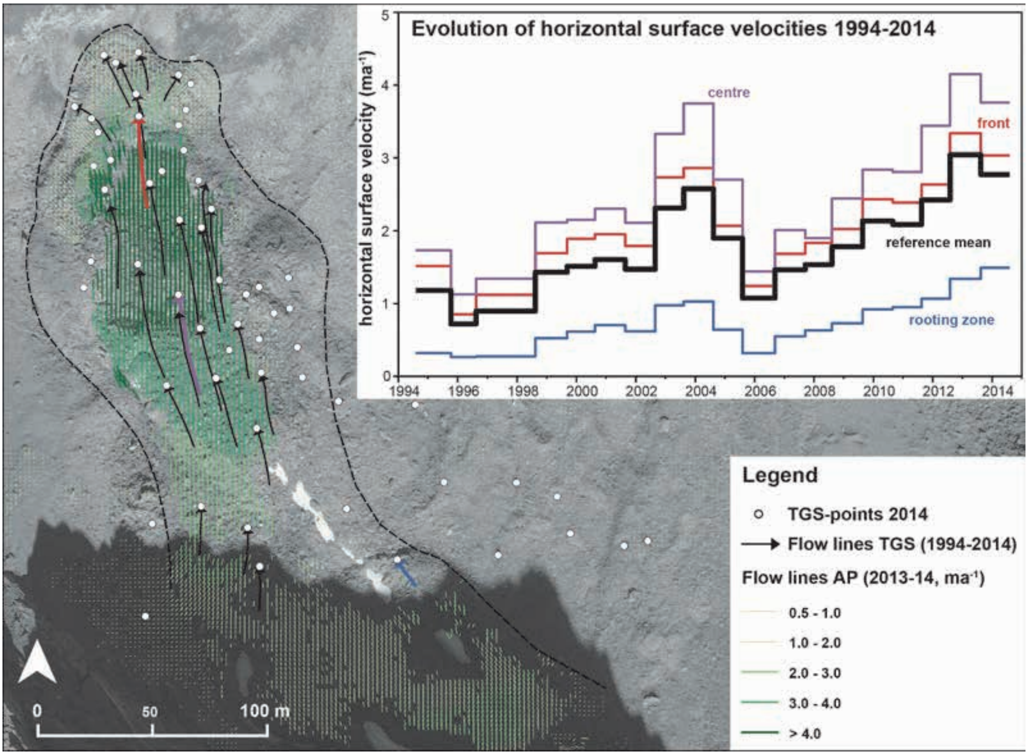

Figure 5.1: *The combination of terrestrial geodetic surveying (TGS) and aerial photogrammetry illustrated with the example of the Gemmi-Furggentälti rock glacier (dashed line). The flow lines in green are based on aerial photographs taken in September 2013 and 2014 and an automatic feature-tracking method (IMCORR, SAGA GIS). At Gemmi, a series of points were surveyed by TGS since 1994 (black lines, white circles) and the fastest zones in the rock glacier centre moved 50–60 m during the past 20 years. The annual velocities quantified by TGS and photogrammetry slightly differ due to different timing of the TGS measurements (mid-August) and the flights (late September). A comprehensive view of spatial and temporal creep variations can be achieved by the combination and systematic repetition of these methods. The underlying orthophoto is based on aerial images taken by Flotron AG (financed by «Förderverein Pro Gemmi») and processed by B. Staub (UniFR). For further information see Krummenacher et al. (2008) and Staub et al. (2015) .*

5.2 Permafrost Creep

Terrestrial geodetic surveys were extended and are currently conducted at 16 rock glacier lobes (cf. Tables 1.1 and A.3 and Figures 1.5 and A.29-A.44). Results are displayed in Table 5.1 and Figure 5.2. In general, ceep velocities dropped until 2006 following the extraordinary high horizontal velocities in 2003 and 2004. Kinematic activity is increasing at most of the sites since 2007. The velocity increase was in the order of +52 % during the reporting period and most rock glaciers reached new velocity maxima in 2014.

Table 5.1: Relative change of the mean horizontal surface velocity (reference values) of PERMOS rock glaciers (comparison to the respective previous year) in percent. The average velocity increase over the entire reporting period 2010–2014 is +52%.

Site	2005	2006	2007	2008	2009	2010	2011	2012	2013	2014
Aget		-22	+23	-28	+44	+3	-7	+5	-1	-5
Corvatsch-Murtèl							+0	+26	-1	+20
Gemmi	-26	-9	-10	+35	+16	-2	-12	+16	+16	-9
Grosses Gufer						-3	-32	+20	+13	+37
Hungerlitälli 1							+4	+17	+11	+21
Hungerlitälli 3	-14	-43	-15	+27	+54	-8	-15	+16	+26	+20
Lapires					+60	+13	-6	+28	+40	+10
Largario							+27	+0	+26	-8
Monte Prosa A							+4	+14	+31	+10
Monte Prosa B							+9	+9	+16	n.a.
Muragl							-7	+2	+18	+31
Réchy		-47	+13	+20	+37	+16	+4	-3	+18	+8
Sceru							+18	+18	+9	+8
Tsarmine		-42	+130	-3	+47	-32	-24	+89	+10	+30
Yettes Condjà B	-52	-54	-4	+29	+82	+36	+0	+11	+39	+44
Yettes Condjà C	-48	+21	-37	+45	+30	+6	+21	-30	+48	-10
Mean	**-35**	**-28**	**+14**	**+18**	**+46**	**+3**	**-1**	**+15**	**+20**	**+14**

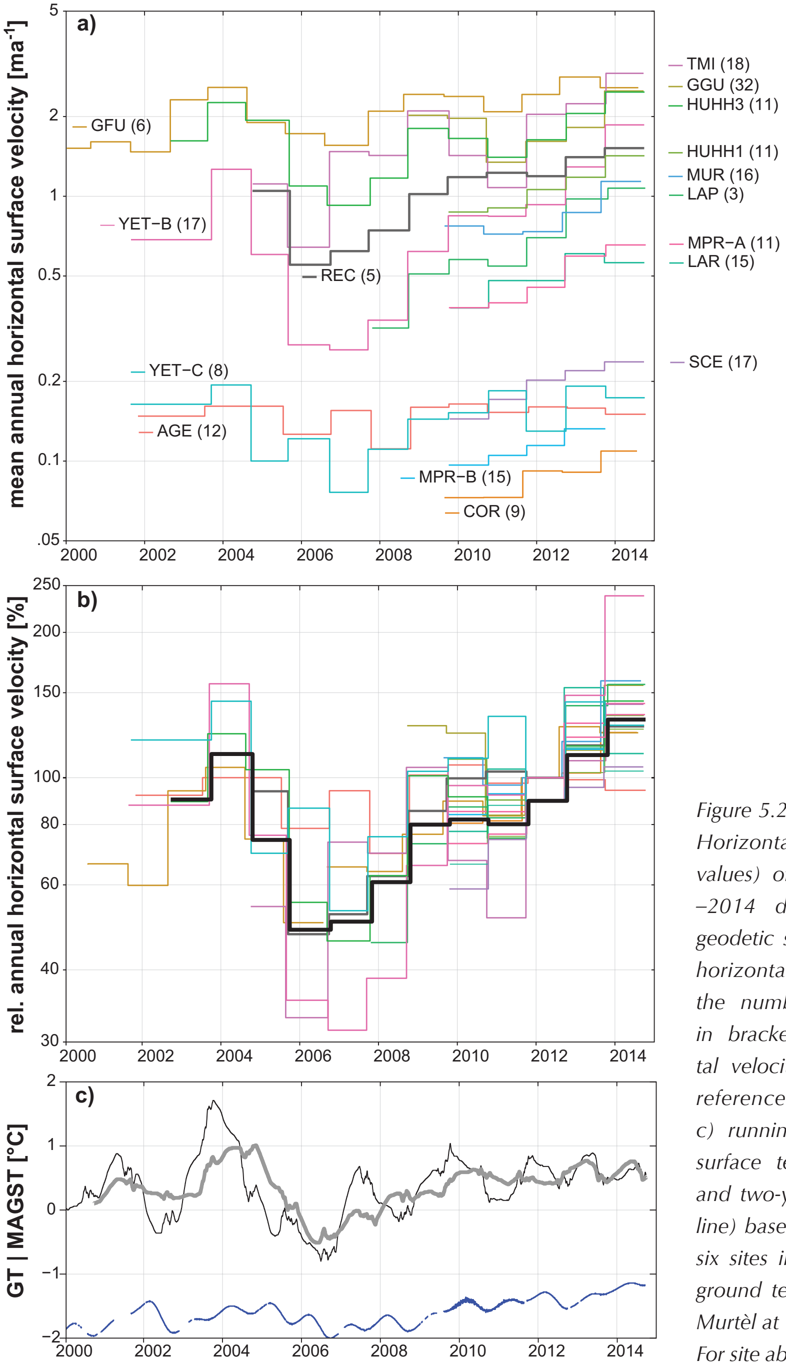

Figure 5.2:
Horizontal velocities (reference values) of 16 rock glaciers 2000–2014 derived from terrestrial geodetic surveys: a) mean annual horizontal velocities (ma^{-1}) for the number of surveyed points in brackets; b) annual horizontal velocities (%) relative to the reference period 2011–2012; c) running mean annual ground surface temperature (black line) and two-year running mean (grey line) based on 36 time series from six sites in Valais and daily mean ground temperature at Corvatsch-Murtèl at 15.5 m depth (blue line). For site abbreviations see Table A.3.

5.3 Rock Fall from Permafrost Areas

A documentation of rock fall events with their detachment zones in permafrost areas was established for PERMOS within the scope of a Master thesis at the UZH and in collaboration with SLF, FOEN, MeteoSwiss and the Swiss Mountain Guide Association (SBV). Basic information on the rock fall events (such as location, date, volume, observation of ice in the detachment zone) is integrated into the documentation when reported and not actively collected. That is, the documentation does not provide a complete inventory and it is therefore observation and registration biased. Nevertheless, the data provided can be used for future analyses like e.g., in Fischer et al. (2012). The documentation is maintained at SLF.

Basic information was collected for twelve events with a known location of the starting zone, year of the event and a volume of at least 1000 m^3. The starting zones were located at an elevation between ca. 2000 and 3500 m asl. (Table 5.2). About eighty events were reported where either the volume, date or exact location of the starting zone was not determined.

On Pizzo Cengalo (Valle Bregaglia) several events occurred on the north face during the reporting period (Figure 5.3). A smaller volume detached in July 2011 followed by a large event of about 1.5 million m^3 (estimated by Swisstopo) in December 2011 from the same area which was almost not noticed (detected by the Swiss Seismological Service). Since the unstable rock mass was expected to be still moving, the hiking path between Capanna di Sciora and Capanna Sasc Furä had to be closed. Later on, a pilot study was started to monitor the rock face in order to better understand the influence of permafrost on large rock slope instabilities. From the accumulation area of the large rock slope failure several debris flows were triggered during heavy precipitation events in summer 2012. To reduce the risk and closing the road an automatic early warning system was established. In autumn 2013, a third event occurred from another part of the rock face.

Table 5.2: Rock fall events from permafrost areas during the reporting period with known starting zone, date and approximate volume.

Location	Date	Elevation	Aspect (m asl.)	Volume (m^3)
Cengalo	19.07.2011	2950	NW	10'000
Piz Lischana	31.07.2011	3100	SE	2'000
Klein Kärpf	August 2011		N	1'700
Birghorn	18.11.2011	2870	N	500'000
Häuselhorn	04.06.2012	2000	S	10'000
Cengalo	27.12.2011	2950	N	1.5 Mio.
Sattelstöckli	26.07.2012	2400	NE	5'000
Sphinx	10.2012	3500	SSE	1'500
Cengalo	24.09.2013	2740	N	100'000
Ober Rotegg	21.05.2014	2650	SW	20'000
Casaccia	23.08.2014	2000	S	2'000–3'000
Piz Kesch	February 2014	3100	N	150'000

Figure 5.3:
Cengalo rock fall in the Val Bregaglia. Overview of the accumulation area, from where several debris flows were triggered (top) and the starting zone (bottom). Photos: J. Nötzli, September 2012.

A detailed description of the collapse of a rock pillar at Piz Kesch in February 2014 can be found in Phillips et al. (2016). According to this publication, it is not possible to distinguish one main triggering factor. However it is likely that ice segregation, frost wedging, glacial loading and unloading and temperature fluctuations all contributed toward fracture propagation.

5.4 Summary

The combination of remote sensing and in-situ measurements allows for the quantification of permafrost creep parameters on various temporal scales. The benefit of the analysis of repeated aerial images is the availability of data for the entire landform, including movement patterns. In addition, vertical changes are quantified independently of the downslope movement and changes related to ice melt or aggradation can be observed. In contrast, by the application of terrestrial methods, annual and seasonal changes can be described and interpreted.

The terrestrial survey now comprise roughly one decade of measurements at most sites, showing distinct inter-annual variations as well as common patterns of relative velocity changes. Since 2007 velocities increased at most sites strongly towards new velocity maxima.

Acknowledgements

PERMOS is financially supported by the Federal Office of Meteorology and Climatology MeteoSwiss in the framework of GCOS Switzerland, the Federal Office for the Environment (FOEN), and the Cryospheric Commission of the Swiss Academy of Sciences (SCNAT).

Installation and maintenance of the various PERMOS sites as well as fieldwork and data preprocessing were performed in the scope of PERMOS or within research projects by the PERMOS partners: The Swiss Federal Institute of Technology (ETH) through their Institute for Geotechnical Engineering (IGT), the WSL Institute for Snow and Avalanche Research (SLF) Davos, the University of Applied Sciences and Arts of Southern Switzerland (SUPSI) through their Institute of Earth Sciences, the University of Lausanne through the Institute of Earth Surface Dynamics, and the Geography Departments of the Universities of Fribourg and Zurich. The contribution and commitment of the partner institutions is indispensable for the development and maintenance of the PERMOS Network.

The present report is a compilation from a number of contributors of data, text, illustrations, and photos, as can be seen in the imprint. In addition, there are numerous field assistants who helped to obtain data as well as generous support from the following companies: Corvatsch-Furtschellas Bahnen, Jungfraubahnen, High Altitude Research Station Jungfraujoch, Schilthorn Bahnen, Andermatt Gotthard Sportbahnen, Téléverbier and Télénendaz.

Finally, our sincere thanks go to all who supported PERMOS in any way and enabled this report.

References

Arenson, L., Hoelzle, M., and Springman, S. M. 2002. Borehole deformation measurements and internal structure of some rock glaciers in Switzerland. Permafrost and Periglacial Processes, 13(2), 117–135. http://doi.org/10.1002/ppp.414.

Begert, M., Frei, C., and Abbt, M. 2013. Einführung der Normperiode 1981–2010, Fachbericht MeteoSchweiz, 245, 50 pp.

Delaloye, R., Lambiel, C., and Gärtner-Roer, I. 2010. Overview of rock glacier kinematics research in the Swiss Alps: seasonal rhythm, interannual variations and trends over several decades. Geographica Helvetica, 65(2), 135–145.

Fischer, L., Purves, R. S., Huggel, C., Noetzli, J., and Haeberli, W. 2012. On the influence of topographic, geological and cryospheric factors on rock avalanches and rockfalls in high-mountain areas. Natural Hazards and Earth System Sciences, 12(1), 241–254. http://doi.org/10.5194/nhess-12-241-2012.

Harris, C., Haeberli, W., Vonder Mühll, D., and King, L. 2001. Permafrost monitoring in the high mountains of Europe: the PACE Project in its global context. Permafrost and Periglacial Processes, 12(1), 3–11. http://doi.org/10.1002/ppp.377.

Hilbich, C. 2009. Geophysical monitoring systems to assess and quantify ground ice evolution in mountain permafrost. University of Jena, Jena, Germany.

Krummenacher, B., Mihajlovic, D., Nussbaum, A. and Staub, B. 2008. 20 Jahre Furggentälti - Permafrostuntersuchungen auf der Gemmi, G80 ed., Geographica Bernensia, Bern.

MeteoSwiss 2010. Das Witterungsjahr 2010, Jahres-Klimabulletin der MeteoSchweiz. Online: URL: http://www.meteoschweiz.admin.ch/web/de/klima/klima_heute/jahresflash/flash2010.html (accessed: May 2012).

MeteoSchweiz 2012. Klimareport 2011. Bundesamt für Meteorologie und Klimatologie MeteoSchweiz, Zürich. 68 S.

MeteoSchweiz 2013. Klimareport 2012. Bundesamt für Meteorologie und Klimatologie MeteoSchweiz, Zürich. 70 S.

MeteoSchweiz 2014. Klimareport 2013. Bundesamt für Meteorologie und Klimatologie MeteoSchweiz, Zürich. 76 S.

MeteoSchweiz 2015. Klimareport 2014. Bundesamt für Meteorologie und Klimatologie MeteoSchweiz, Zürich. 80 S.

PERMOS 2013. Permafrost in Switzerland 2008/2009 and 2009/2010. Noetzli, J. (ed), Glaciological Report (Permafrost) No. 10/11 of the Cryospheric Commission (CC) of the Swiss Academy of Sciences (SCNAT), 80 pp.

Phillips, M., Wolter, A., Lüthi, R., Amann, F., Kenner, R., and Buhler, Y. 2016. Rock slope failure in a recently deglaciated permafrost rock wall at Piz Kesch (Eastern Swiss Alps), February 2014. Earth Surface Processes and Landforms, 1–13. http://doi.org/10.1002/esp.3992

Staub, B., Vogel, D., Budmiger, K., Krummenacher, B., Delaloye, R. and Kienholz, H. 2015. Einsatz der Photogrammetrie und Bildanalyse zur Quantifizierung von Blockgletscherbewegungen, Geomatik Schweiz, 113(9), 356–361.

Staub B., Hasler, A., Noetzli, J., and Delaloye, R. 2016. Gap filling algorithm for ground surface temperature data, Permafrost and Periglacial Processes. http://doi.org/10.1002/ppp.1913.

Wirz, V., Geertsema, M., Gruber, S., and Purves, R. S. 2015. Temporal variability of diverse mountain permafrost slope movements derived from multi-year daily GPS data, Mattertal, Switzerland. Landslides. http://doi.org/DOI 10.1007/s10346-014-0544-3.

Appendix

PERMOS Boreholes

Table A.1a: Location and characteristics of the boreholes.

Borehole	Region	Morphology	Y CH1903	X CH1903	Elev. (m a.s.l.)	Slp. (°)	Asp.	Surface mat.
Corvatsch-Murtèl 0200	Engadine	Rock glacier	783175	144692	2672	10	NW	Coarse blocks
Corvatsch-Murtèl 0287	Engadine	Rock glacier	783160	144720	2670	10	NW	Coarse blocks
Dreveneuse 0104	Chablais	Talus slope	557670	124805	1580	30	E	Coarse blocks
Flüela 0102	Engadine	Talus slope	791375	180575	2394	26	NE	Debris
Gemsstock 0106	Urner Alps	Crest	689781	161780	2940	50	NW	Bedrock
Gentianes 0102	Lower Valais	Moraine	589467	103586	2888	20	E	Debris
Jungfraujoch 0195	Bernese Oberland	Crest	641000	155120	3590	55	N	Bedrock
Lapires 0198	Lower Valais	Talus slope	588070	106080	2500	25	NE	Coarse blocks
Lapires 1108	Lower Valais	Talus slope	588099	106092	2500	25	NE	Coarse blocks
Lapires 1208	Lower Valais	Talus slope	588028	106027	2535	25	NE	Coarse blocks
Les Attelas 0108	Lower Valais	Talus slope	587196	105043	2661	30	W	Coarse blocks
Les Attelas 0208	Lower Valais	Talus slope	587243	105040	2689	30	W	Debris
Matterhorn 0205	Upper Valais	Crest	618399	92334	3295	0	–	Bedrock
Muot da Barba Peider 0196	Engadine	Talus slope	791314	152493	2946	38	NW	Debris
Muot da Barba Peider 0296	Engadine	Talus slope	791339	152513	2941	38	NW	Debris
Muragl 0199	Engadine	Rock glacier	791025	153726	2536	15	NW	Coarse blocks
Muragl 0299	Engadine	Rock glacier	790989	153687	2539	15	NW	Coarse blocks
Muragl 0499	Engadine	Rock glacier	791017	153688	2549	15	SW	Coarse blocks
Ritigraben 0105	Upper Valais	Rock glacier	631755	113775	2690	0	–	Coarse blocks
Schafberg 0190	Engadine	Rock glacier	790944	152590	2754	0	–	Coarse blocks
Schafberg 0290	Engadine	Rock glacier	790855	152745	2732	0	–	Coarse blocks
Schilthorn 5198	Bernese Oberland	Crest	630365	156410	2909	30	NE	Debris
Schilthorn 5000	Bernese Oberland	Crest	630350	156410	2910	30	NE	Debris
Schilthorn 5200	Bernese Oberland	Crest	630350	156410	2910	30	NE	Debris
Stockhorn 6000	Upper Valais	Crest	629878	92876	3410	8	S	Debris
Stockhorn 6100	Upper Valais	Crest	629867	92850	3410	8	S	Debris
Tsaté 0104	Lower Valais	Crest	608490	106400	3040	30	W	Bedrock

Table A.1b: Instrumentation of the boreholes.

Borehole	Since	Depth	Lowest S.	#Therm.	Sensors	Access	Calib.	Institution
	(m)	(m)						
Corvatsch-Murtèl 0200	2000	63.20	62.00	30	YSI 44006	remote	2000	ETHZ
Corvatsch-Murtèl 0287	1987	62.00	57.95	46	YSI 44006	remote	1997	UZH
Dreveneuse 0104	2004	15.00	14.50	12	MAAD	on site	2006	UNIFR
Flüela 0102	2002	23.00	20.00	12	YSI 46006	on site	2002	SLF
Gemsstock 0106	2006	40.00	39.50	27	YSI 44008	on site	2005	SLF
Gentianes 0102	2002	20.04	20.04	11	MAAD	on site	2002	UNIL
Jungfraujoch 0195	1995	19.7	19.70	9	YSI 46008	remote	2009	SLF
Lapires 0198	1998	19.60	19.60	12	YSI 44031	remote	1998	UNIFR
Lapires 1108	2008	40.00	39.00	28	YSI 44031	remote	2008	UNIFR
Lapires 1208	2008	35.00	34.00	18	YSI 44031	remote	2008	UNIFR
Les Attelas 0108	2008	26.00	24.00	12	MAAD	on site	2008	UNIL
Les Attelas 0208	2008	21.00	20.00	11	MAAD	on site	2008	UNIL
Matterhorn 0205	2005	53.00	52.90	12	YSI 44008	on site	2005	SLF
Muot da Barba Peider 0196	1996	18.00	17.50	10	YSI 44008	on site	1996	SLF
Muot da Barba Peider 0296	1996	18.00	17.50	10	YSI 44008	on site	1996	SLF
Muragl 0199	1999	70.20	69.70	18	YSI 44006	on site	1999	ETHZ
Muragl 0299	1999	64.00	60.00	22	YSI 44006	on site	1999	ETHZ
Muragl 0499	1999	72.00	69.59	22	YSI 44006	on site	1999	ETHZ
Ritigraben 0105	2002	30.00	14.00	30	YSI 44006	remote	2002	SLF
Schafberg 0190	1990	67.00	15.90	15	YSI 46006	on site	2005	SLF
Schafberg 0290	1990	37.00	25.20	10	YSI 46006	on site	1997	SLF
Schilthorn 5198	1998	14.00	13.00	14	YSI 44006	remote	1998	UZH
Schilthorn 5000	2000	101.00	100.00	30	YSI 44006	remote	1999	UZH
Schilthorn 5200	2000	100.00	87.00	19	YSI 44006	remote	1999	UZH
Stockhorn 6000	2000	100.00	98.30	30	YSI 44006	remote	2000	UNIFR
Stockhorn 6100	2000	31.00	17.00	18	YSI 44006	remote	2000	UNIFR
Tsaté 0104	2004	20.00	19.50	11	MAAD	on site	2006	UNIL

Active Layer Depths

Table A.2a: Depth and date of maximum active layer thickness in the borehole COR_0287 1988–1996.

Year	1987	1988	1989	1990	1991	1992	1993	1994	1995	1996
ALT	3.4	3.2	3.1	3.3	3.4	3.4	3.5	3.5	3.4	3.4
Date	24.09	03.08	01.10	01.09	23.09	28.08	23.08	12.09	16.08	29.08

Table A.2b: Depth and date of maximum active layer thickness in the boreholes 1997–1999.

Name	1997		1998		1999	
	ALT	Date	ALT	Date	ALT	Date
COR_0287	3.4	15.09	3.5	21.08	3.4	31.08
LAP_0198					3.7	07.10
MBP_0196	0.7	10.09	0.9	22.08	0.9	19.09
MBP_0296	1.7	16.09	1.9	24.08	1.9	19.09
SBE_0290	3.2	18.08	3.2	14.08	3.2	28.08
SCH_5198			4.3	01.11	4.4	10.10

Table A.2c: Depth and date of maximum active layer thickness in the boreholes 2000–2007.

Name	2000		2001		2002		2003		2004		2005		2006		2007	
	ALT	Date	ALT	Date	ALT	Date	ALT	Date	ALT	Date	ALT	Date	ALT	Date	ALT	Date
COR_0200	–	–	–	–	3.4	03.09	3.2	31.08	2.9	13.09	2.5	05.09	2.5	14.09	2.5	16.08
COR_0287	3.5	30.08	3.5	05.09	3.4	05.09	3.5	24.08	3.5	07.09	3.5	08.09	3.5	13.09	3.5	22.08
FLU_0102	–	–	–	–	–	–	3.0	26.08	2.9	13.09	2.9	18.09	3.0	25.09	3.0	01.09
GEN_0102	–	–	–	–	–	–	1.4	30.08	1.4	14.09	1.5	05.09	1.4	05.10	1.5	26.09
LAP_0198	3.8	14.10	3.9	15.09			4.4	01.10	4.5	15.10	4.6	15.10.			4.6	20.10
MAT_0205	–	–	–	–	–	–	–	–	–	–	–	–	3.2	06.08	3.3	08.09
MBP_0196	0.7	18.09	0.8	30.08	0.8	09.09	1.6	01.09	1.0	17.09	1.0	12.09	1.1	06.10	1.0	01.09
MBP_0296	1.9	01.09	1.9	31.08	1.9	09.09	2.4	17.09	2.2	21.09	2.0	14.09	2.0	29.09	2.0	05.09
MUR_0499	–	–	3.5	03.09	3.3	08.09	3.5	04.09	4.2	05.10	4.4	22.09	4.5	06.09	4.5	16.09
RIT_0105	–	–	–	–	–	–	–	–	–	–	4.4	02.10	4.3	23.09	4.1	04.09
SBE_0190	–	–	–	–	–	–	–	–	–	–	3.9	08.09	3.9	16.09	4.0	20.08
SBE_0290	5.0	04.09	5.0	12.09	4.9	08.09	5.1	30.08	5.0	18.09	5.0	14.09	4.9	05.10	5.0	24.08
SCH_5000	–	–	–	–	3.0	23.10	8.3	06.11	4.8	28.09	3.7	09.10	3.7	07.10	3.1	04.10
SCH_5198	4.9	06.10	–	–	4.6	01.10	9.0	28.10	4.8	06.10	4.8	06.10	4.8	20.10	4.7	09.10
SCH_5200	–	–	–	–	–	–	3.0	31.10	3.3	08.10	2.3	18.09	1.3	26.09	1.2	09.10
STO_6000	–	–	–	–	2.9	20.09	4.3	20.10	3.7	20.09	–	–	3.1	20.09	–	–
STO_6100	–	–	–	–	3.4	20.09	4.1	20.10	3.9	20.10	–	–	3.5	20.09	–	–
TSA_0104	–	–	–	–	–	–	–	–	–	–	6.5	22.10	–	–	6.5	30.10

Table A.2d: Depth and date of maximum active layer thickness in the boreholes 2008–2014.

Name	2008		2009		2010		2011		2012		2013		2014	
	ALT	Date	ALT	Date	ALT	Date	ALT	Date	ALT	Date	ALT	Date	ALT	Date
ATT_0108	–	–	3.9	06.09	3.8	27.08	3.9	08.09	3.9	25.08	3.9	08.09	3.9	16.10
ATT_0208	–	–	5.8	29.08	5.0	25.08	5.0	20.08	5.0	15.08	5.4	29.09	5.0	08.09
COR_0200	2.5	06.09	2.5	03.09	2.4	24.08	2.5	06.09	2.4	24.08	2.5	09.09	2.5	11.10
COR_0287	3.5	04.09	3.5	08.09	3.5	26.08	3.8	06.10	4.1	06.10	4.2	25.09	4.2	02.09
FLU_0102	3.0	14.09	3.0	01.09	2.9	29.08	3.0	17.09	3.0	24.08	3.0	07.09	3.0	29.08
GEN_0102	–	–	2.1	02.10	2.0	25.09	3.1	20.10	3.0	08.10	4.0	12.12	4.4	17.12
LAP_0198	–	–	5.1	07.10	5.1	01.10	5.2	24.09	5.2	11.10	5.2	26.10	5.2	13.10
LAP_1108	–	–	4.8	09.19	4.4	12.10	4.6	08.10	4.8	08.10	5.3	21.11	–	–
LAP_1208	–	–	–	–	4.4	13.09	4.6	08.10	4.5	24.09	4.6	09.10	4.7	19.09
MAT_0205	2.9	17.09	3.7	01.10	3.0	03.09	3.6	20.09	3.4	15.09	3.4	10.09	2.7	13.09
MBP_0196	1.0	15.09	1.0	28.09	–	–	–	–	–	–	–	–	–	–
MBP_0296	2.1	22.09	2.0	04.10	2.0	04.09	–	–	–	–	–	–	–	–
MUR_0499	–	–	4.5	20.08	4.5	05.09	4.6	18.08	4.6	19.08	4.5	22.06	–	–
RIT_0105	3.8	07.09	3.7	08.10	3.4	29.08	3.4	16.09	3.5	15.09	–	–	3.2	23.09
SBE_0190	4.0	07.09	4.1	04.11	–	–	–	–	–	–	–	–	–	–
SBE_0290	5.0	16.09	5.1	05.09	5.1	03.09	5.2	22.09	5.1	30.08	5.1	10.09	5.1	21.08
SCH_5000	3.9	13.09	7.2	21.11	–	–	6.8	28.09	6.8	08.09	6.9	26.10	8.9	18.10
SCH_5198	5.0	25.09	7.0	23.10	6.8	20.09	6.7	10.10	6.9	26.11	7.7	17.11	4.9	19.10
SCH_5200	1.9	17.09	3.0	01.11	2.9	21.09	2.9	27.09	3.3	10.10	3.2	26.10	2.9	20.10
STO_6000	3.3	15.09	–	–	3.3	27.09	4.0	10.10	3.7	26.09	3.5	16.09	3.3	13.10
STO_6100	3.4	23.09	4.4	28.11	4.5	03.12	4.6	03.12	4.7	08.12	4.8	14.12	4.8	06.12
TSA_0104	6.4	03.10	7.0	26.10	6.8	06.10	6.9	21.11	7.7	16.09	7.7	18.09	7.3	18.10

Attelas 0108

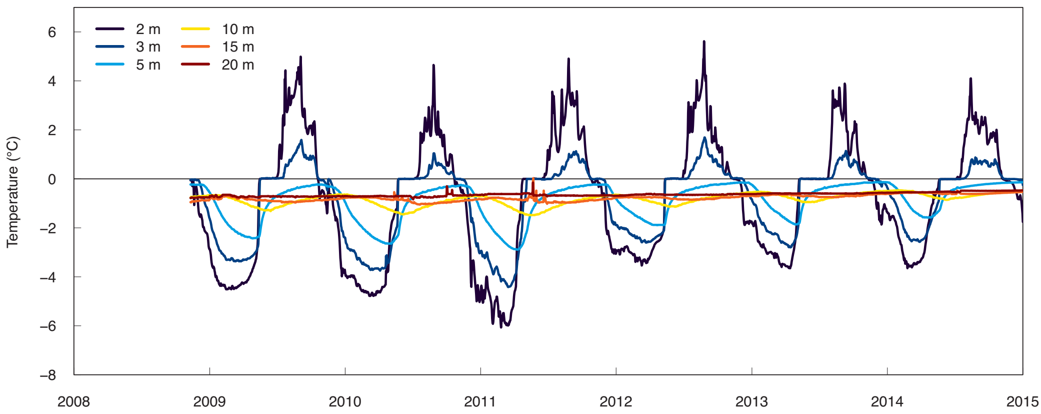

Figure A.1: Temperature-time series measured in the Attelas 0108 borehole.

Attelas 0208

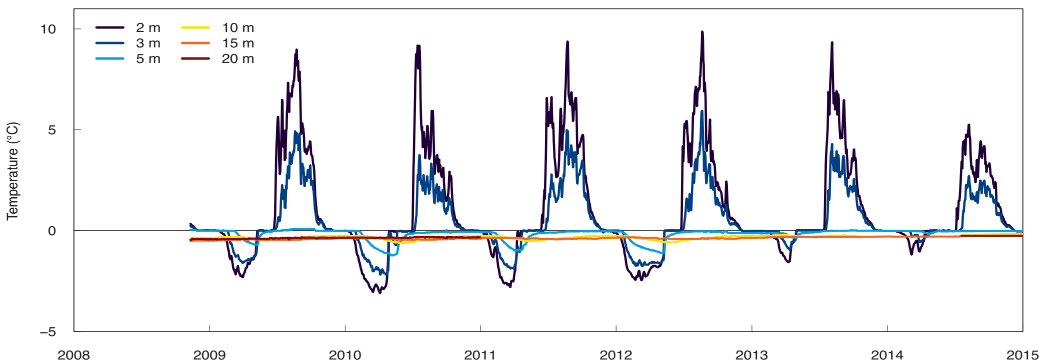

Figure A.2: Temperature-time series measured in the Attelas 0208 borehole.

Corvatsch-Murtèl 0287

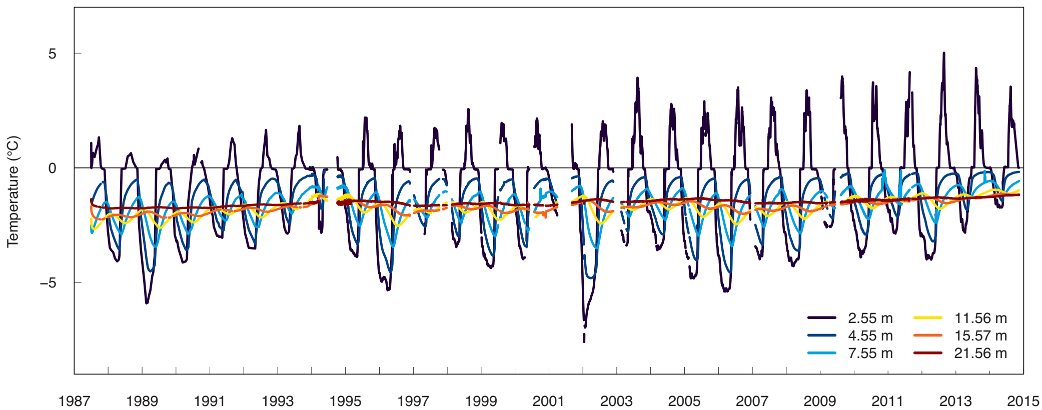

Figure A.3: *Temperature-time series measured in the Murtèl-Corvatsch 0287 borehole.*

Corvatsch-Murtèl 0200

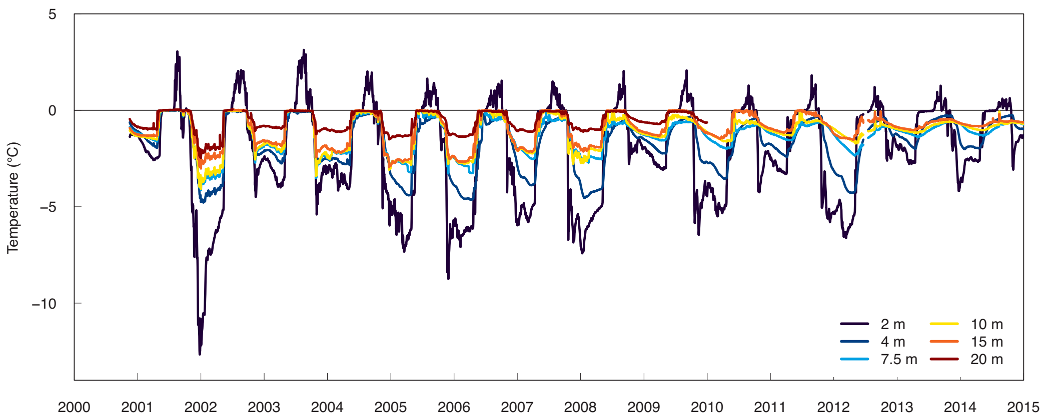

Figure A.4: *Temperature-time series measured in the Murtèl-Corvatsch 0200 borehole.*

Dreveneuse 0104

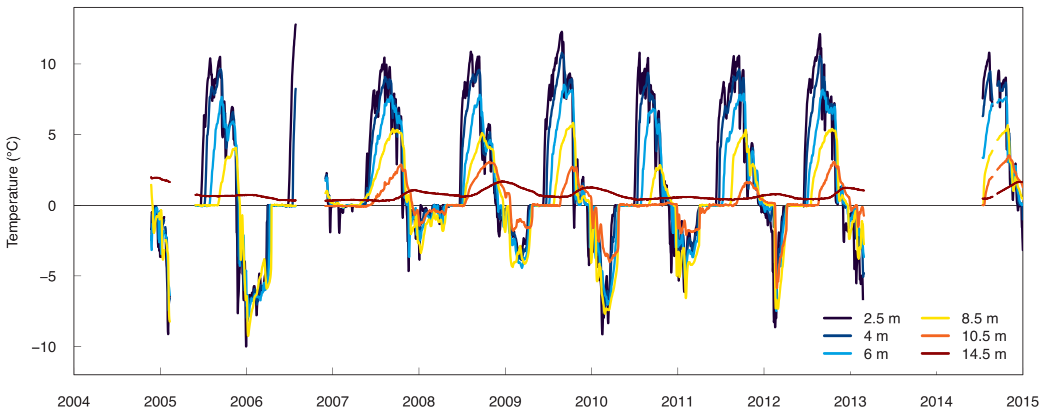

Figure A.5: Temperature-time series measured in the Dreveneuse 0104 borehole.

Flüela 0102

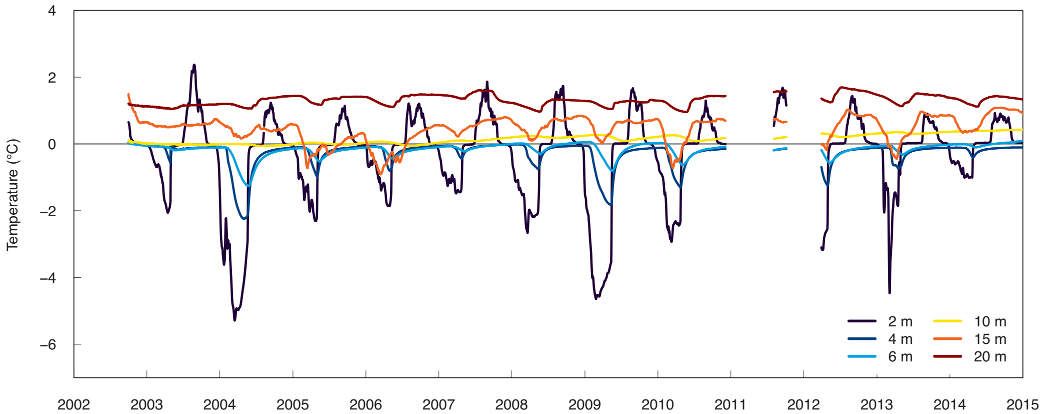

Figure A.6: Temperature-time series measured in the Flüela 0102 borehole.

Gemsstock 0106

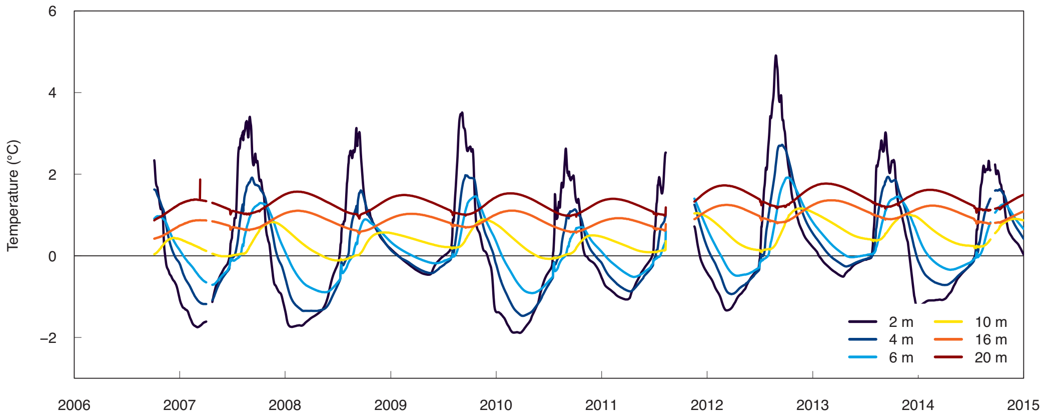

Figure A.7: *Temperature-time series measured in the Gemsstock 0106 borehole.*

Gentianes 0102

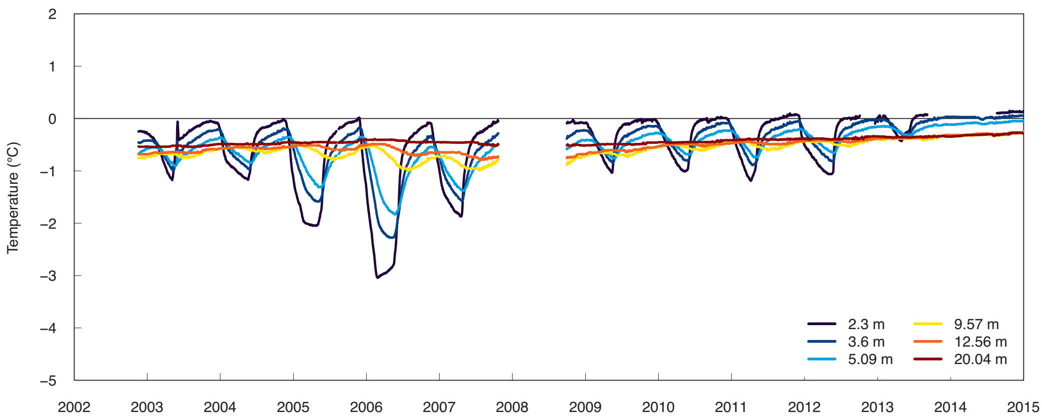

Figure A.8: *Temperature-time series measured in the Gentianes 0102 borehole.*

Jungfraujoch 0195

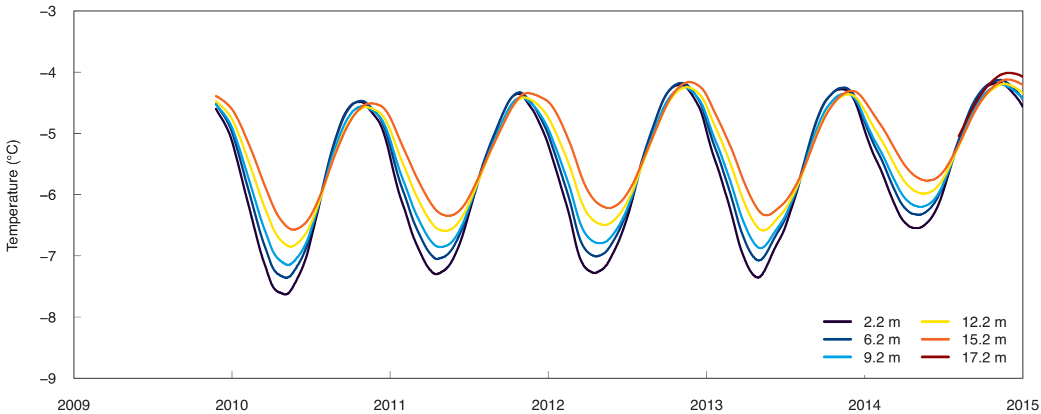

Figure A.9: Temperature-time series measured in the Jungfraujoch 0195 borehole.

Lapires 0198

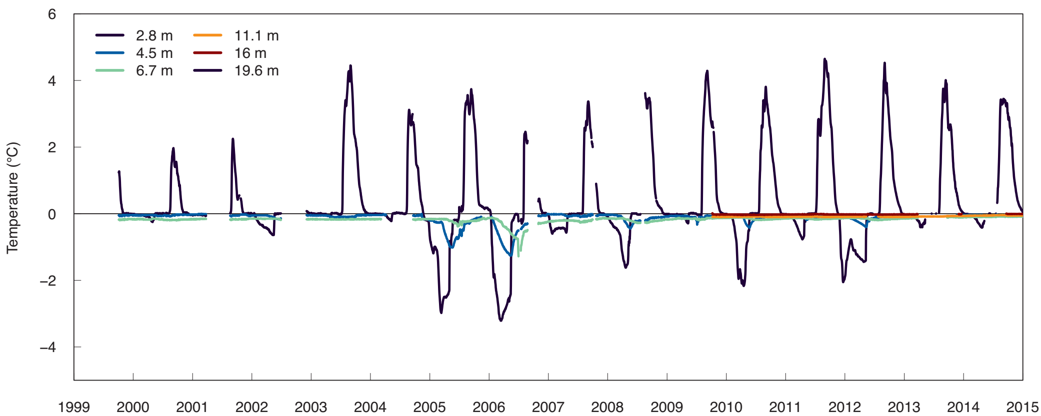

Figure A.10: Temperature-time series measured in the Lapires 0189 borehole.

Lapires 1108

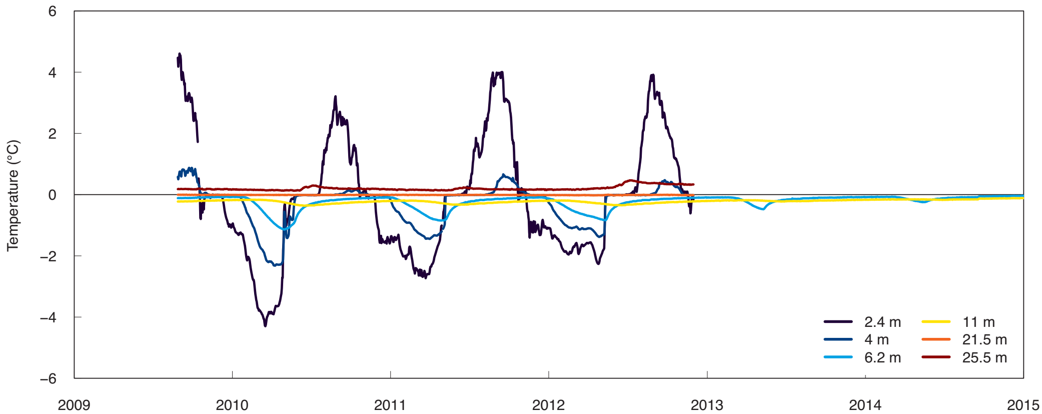

Figure A.11: *Temperature-time series measured in the Lapires 1108 borehole.*

Lapires 1208

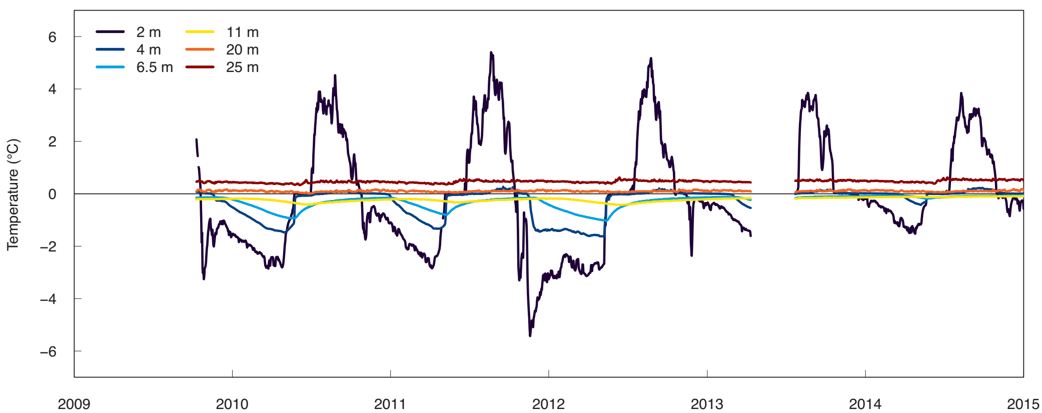

Figure A.12: *Temperature-time series measured in the Lapires 1208 borehole.*

Matterhorn 0205

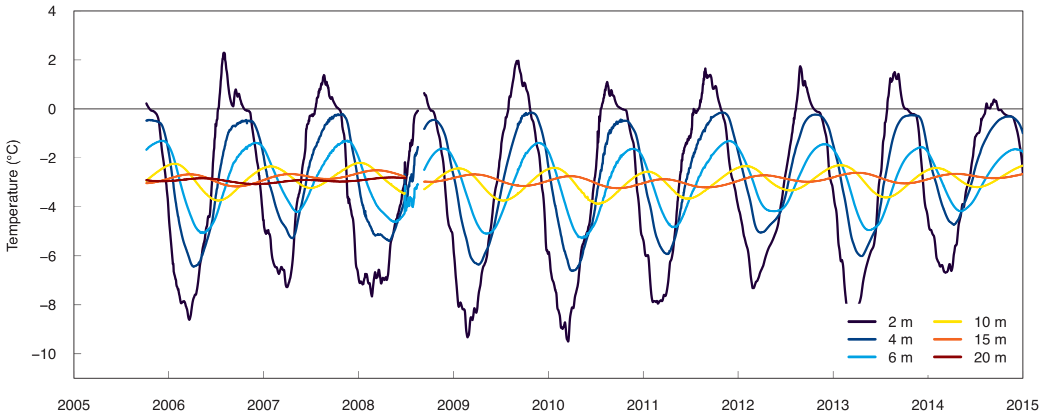

Figure A.13: *Temperature-time series measured in the Matterhorn 0205 borehole.*

Muot Da Barba Peider 0196

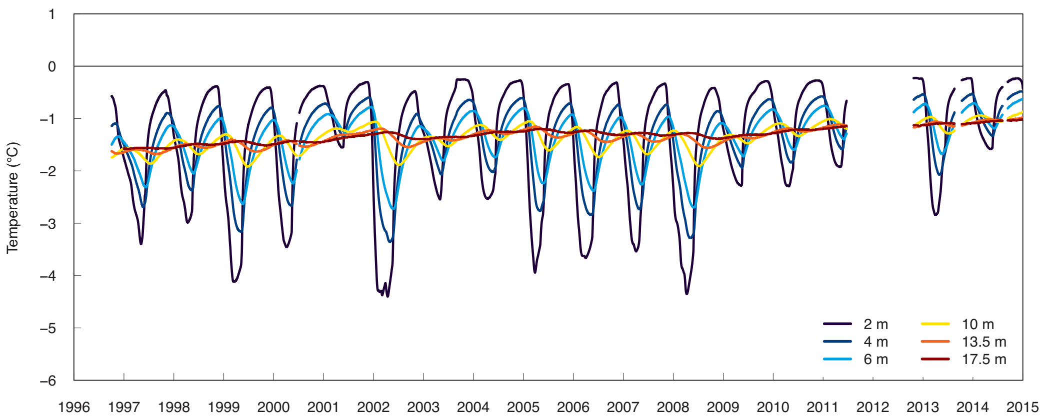

Figure A.14: *Temperature-time series measured in the Muot Da Barba Peider 0196 borehole.*

Muot Da Barba Peider 0296

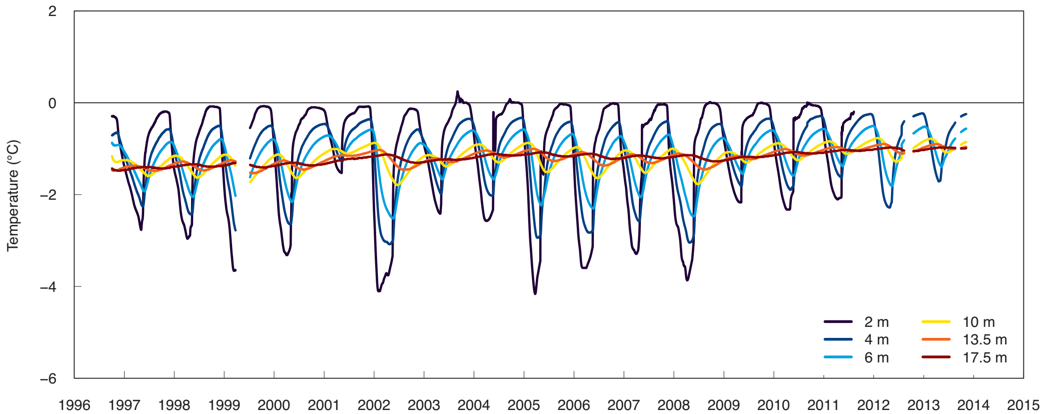

Figure A.15: Temperature-time series measured in the Muot Da Barba Peider 0296 borehole.

Muragl 0199

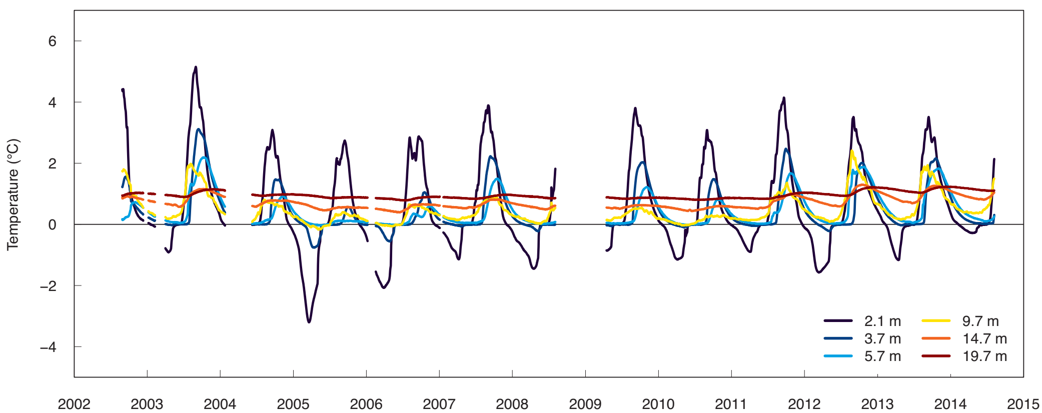

Figure A.16: Temperature-time series measured in the Muragl 0199 borehole.

Muragl 0299

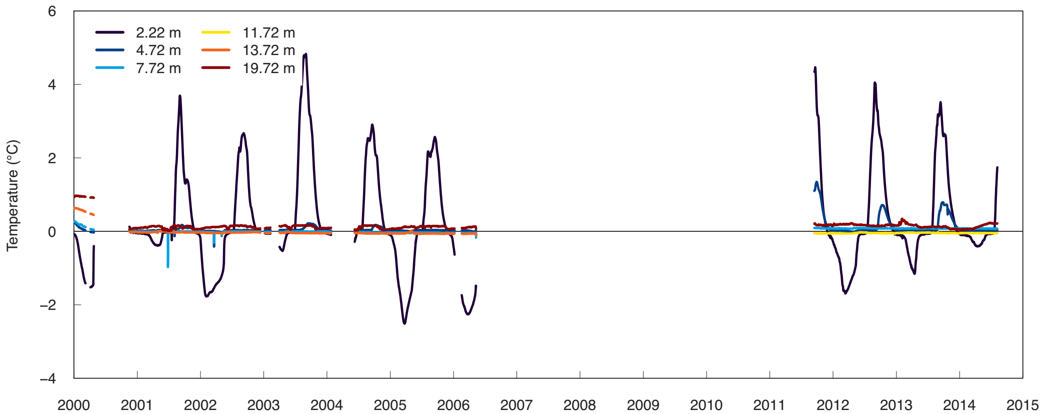

Figure A.17: Temperature-time series measured in the Muragl 0299 borehole.

Muragl 0499

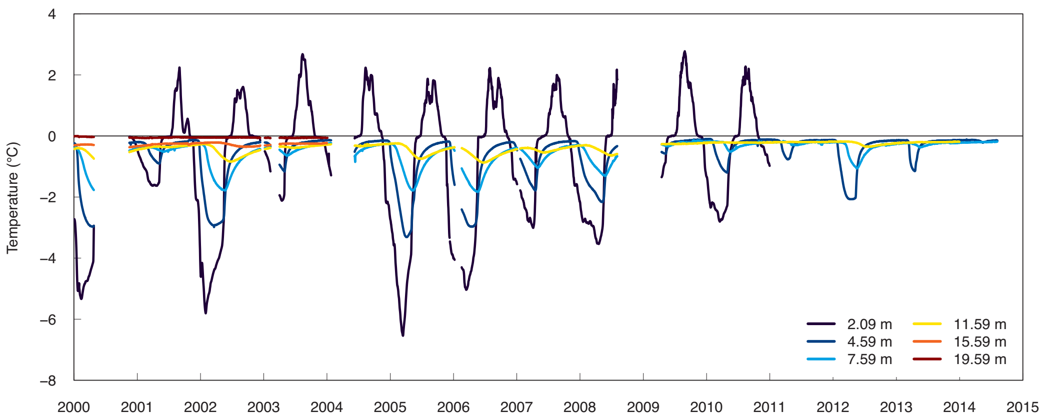

Figure A.18: Temperature-time series measured in the Muragl 0499 borehole.

Ritigraben 0102

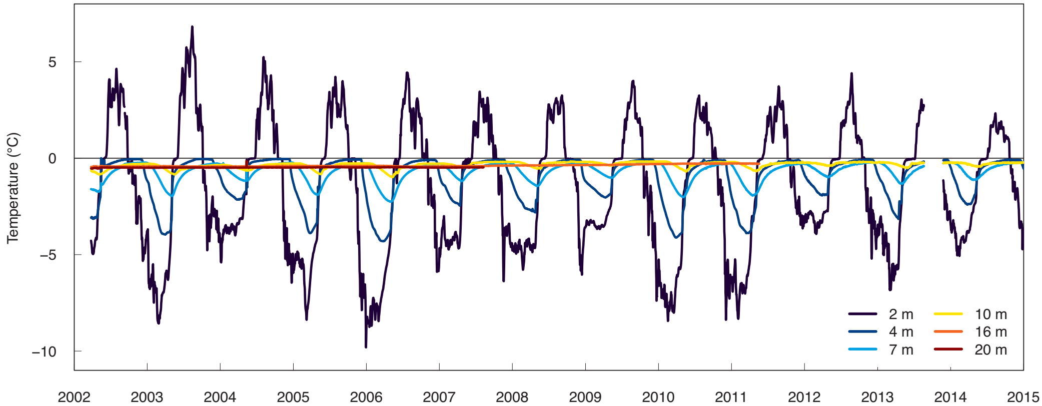

Figure A.19: *Temperature-time series measured in the Ritigraben 0102 borehole.*

Schafberg 0190

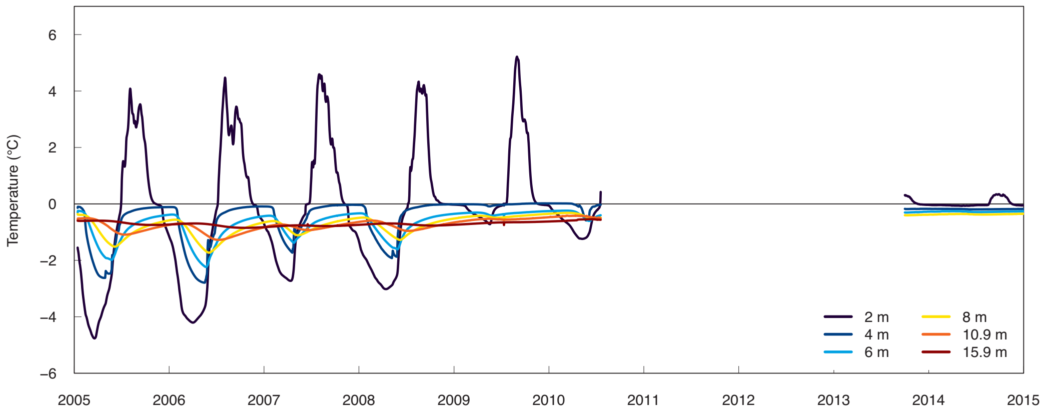

Figure A.20: *Temperature-time series measured in the Schafberg 0190 borehole.*

Schafberg 0290

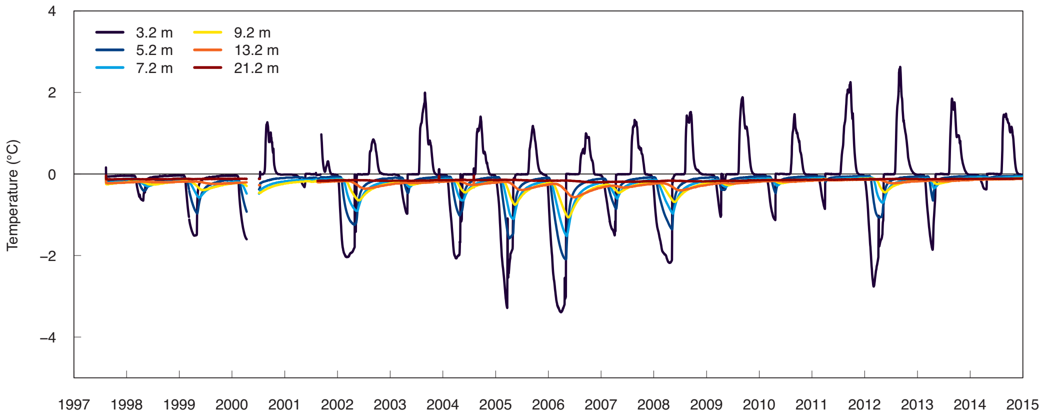

Figure A.21: Temperature-time series measured in the Schafberg 0290 borehole.

Schilthorn 5198

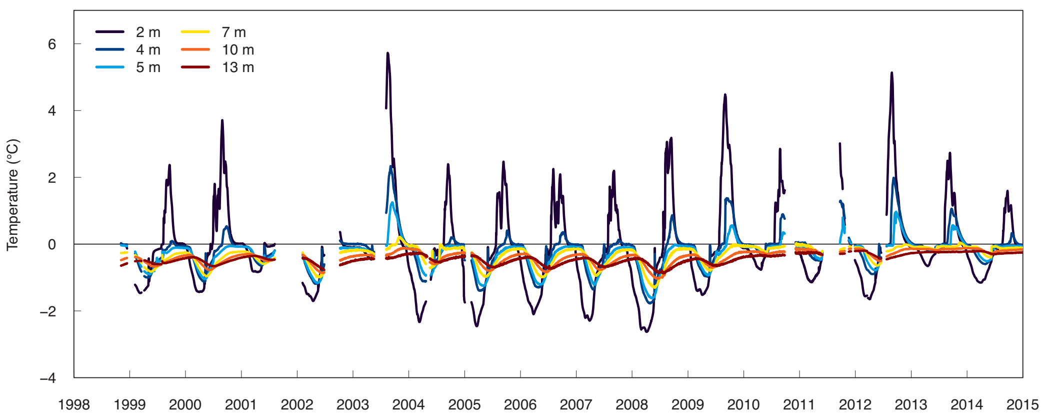

Figure A.22: Temperature-time series measured in the Schilthorn 5198 borehole.

Schilthorn 5000

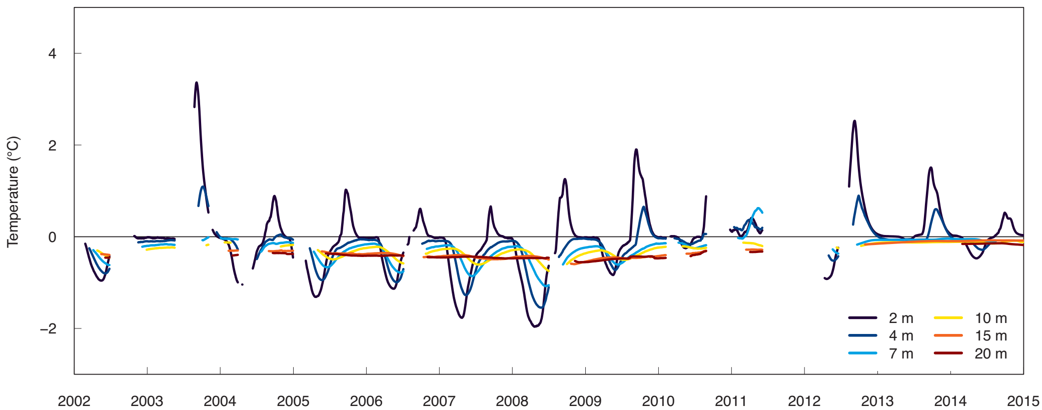

Figure A.23: *Temperature-time series measured in the Schilthorn 5000 borehole.*

Schilthorn 5200

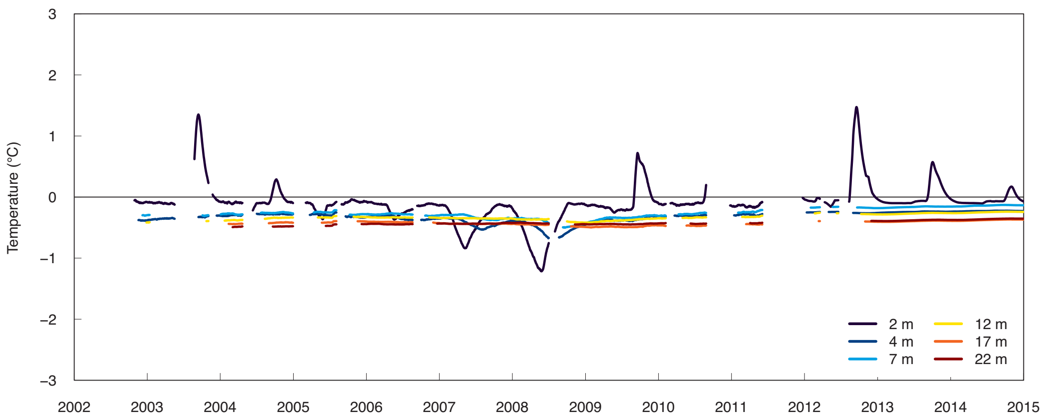

Figure A.24: *Temperature-time series measured in the Schilthorn 5200 borehole.*

Stockhorn 6000

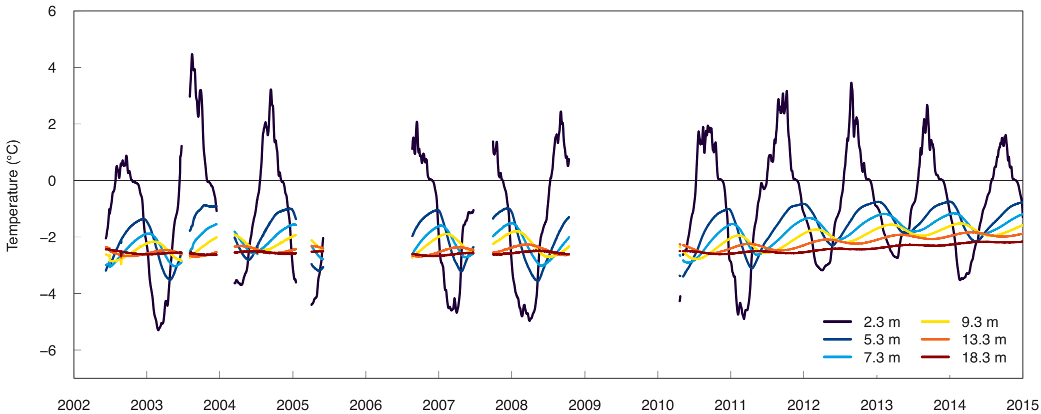

Figure A.25: *Temperature-time series measured in the Stockhorn 6000 borehole.*

Stockhorn 6100

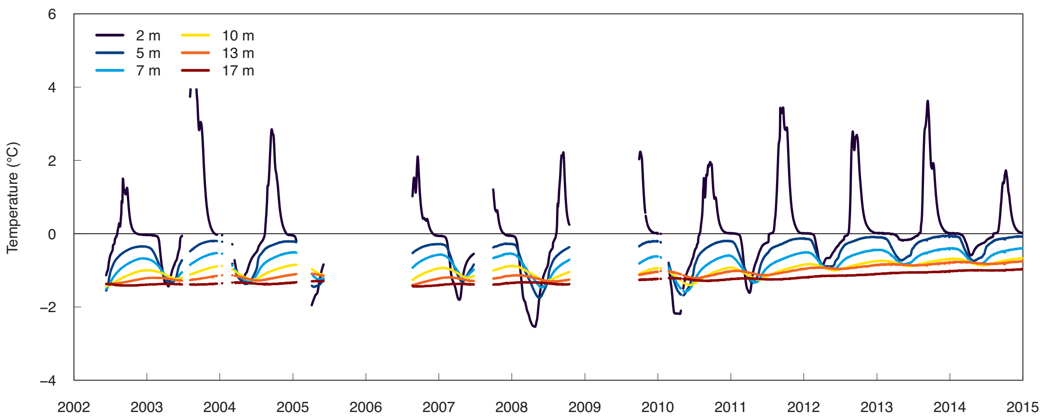

Figure A.26: *Temperature-time series measured in the Stockhorn 6100 borehole.*

Tsaté 0104

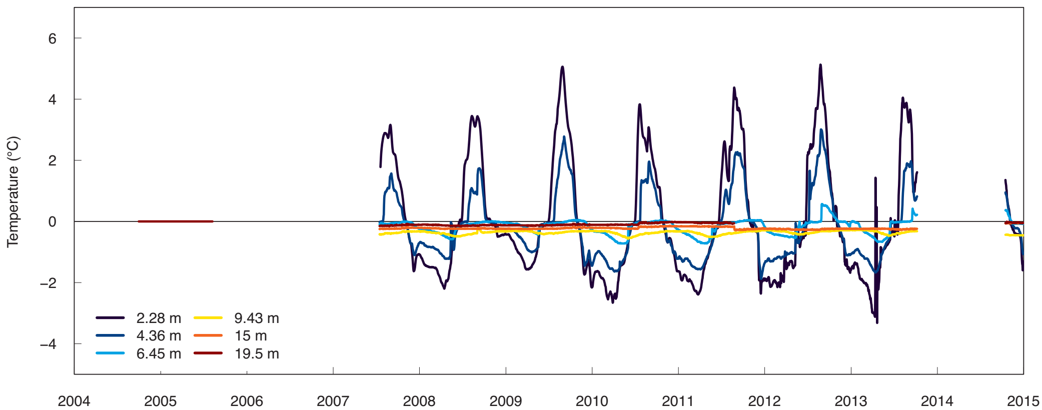

Figure A.27: *Temperature-time series measured in the Tsaté 0104 borehole.*

PERMOS Kinematics Sites

Table A.3: Rock glaciers where terrestrial surveys are conducted.

Site	Region	Aspect	Elevation (m a.s.l.)	Start	Institution
Aget (AGE)	Lower Valais	SE	2810–2890	2001	UniFR
Alpage de Mille (MIL)	Lower Valais	NE	2230–2450	2009	UniFR
Gemmi (GFU)	Bernese Oberland	N	2450–2650	1994	UniFR
Grosses Gufer (GGU)	Bernese Oberland	NW	2360–2600	2007	UniFR
Hungerlitälli 1 (HUHH1)	Lower Valais	NNW	2630–2780	2001	UZH
Hungerlitälli 3 (HUHH3)	Lower Valais	NW	2515–2650	2002	UZH
Lapires (LAP)	Lower Valais	NNE	2640–2610	2007	UniFR
Monte Prosa A (MPR-A)	Ticino	N	2430–2600	2009	UniFR
Monte Prosa B (MPR-B)	Ticino	WNW	2450–2520	2009	UniFR
Corvatsch-Murtèl (COR)	Engadine	NW	2630–2800	2009	UZH
Muragl (MUR)	Engadine	NW	2490–2750	2009	UZH
Réchy (REC)	Lower Valais	NW	2610–2850	2001	UniFR
Stabbio di Largario (LAR)	Ticino	N	2240–2550	2009	SUPSI
Tsarmine (TMI)	Lower Valais	W	2460–2640	2004	UniFR/UniL
Valle di Sceru (SCE)	Ticino	NE	2450–2550	2009	SUPSI
Yettes Condjà B (YET-B)	Lower Valais	NE	2600–2740	2000	UniL
Yettes Condjà C (YET-C)	Lower Valais	NE	2620–2820	2000	UniL

Kinematics Aget

Location: Aget (Lower Valais) | Type: push-moraine | Lithology: quartzite

Area (km^2):	0.05
Length (m):	175
Width (m):	350
Rooting zone (m asl.):	2890
Front (m asl.):	2810
Average slope (°):	13
Exposition:	SE

Method(s): dGPS
Number of points (ref.): 95 (12)
Measurement begin: 2001
Institution: UniFR

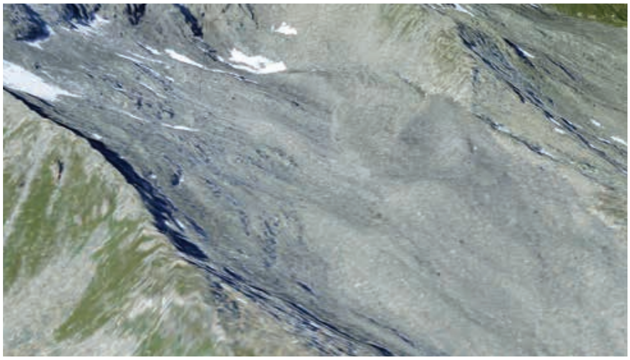

Source: Swiss Federal Office of Topography swisstopo

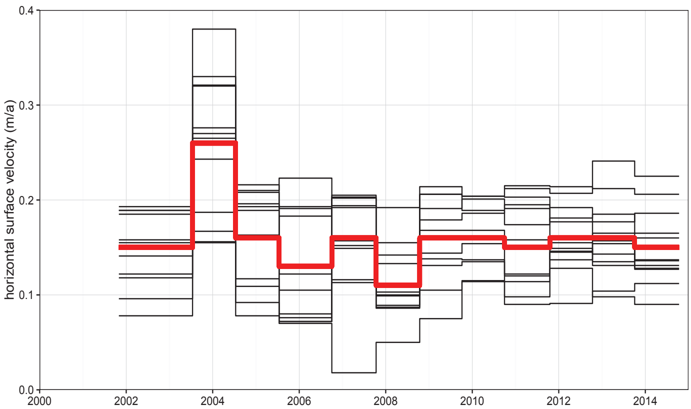

Figure A.28: Annual horizontal surface velocities at the Aget kinematics site for individual points and the mean of the reference points (12, red line).

Kinematics Alpage de Mille

Location: Alpage de Mille (Lower Valais) | Type: rock glacier | Lithology: gneiss

Area (km^2):	0.02
Length (m):	230
Width (m):	90
Rooting zone (m asl.):	2440
Front (m asl.):	2350
Average slope (°):	18
Exposition:	NE

Method(s): dGPS
Number of points (ref.): 85 (9)
Measurement begin: 2003
Institution: UniFR

Photo: Reynald Delaloye

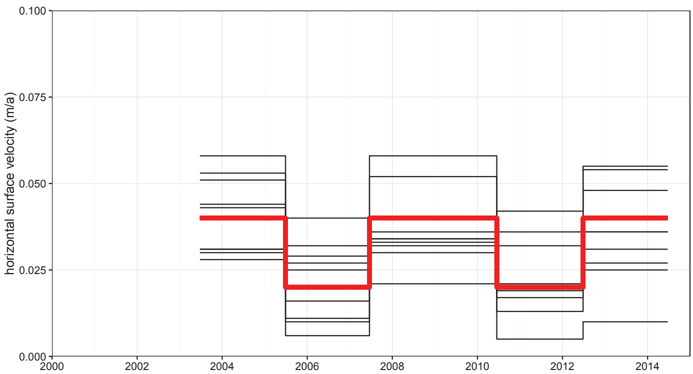

Figure A.29: Annual horizontal surface velocities at the Alpage de Mille kinematics site for individual points and the mean of the reference points (9, red line).

Kinematics Gemmi

Location: Gemmi (Bernese Oberland) | Type: rock glacier | Lithology: limestone

Area (km^2):	0.04
Length (m):	330
Width (m):	130
Rooting zone (m asl.):	2600
Front (m asl.):	2450
Average slope (°):	25
Exposition:	N

Method(s): TGS (until 2011), dGPS
Number of points (ref.): 33 (6)
Measurement begin: 1994
Institution: UniFR

Photo: Benno Staub

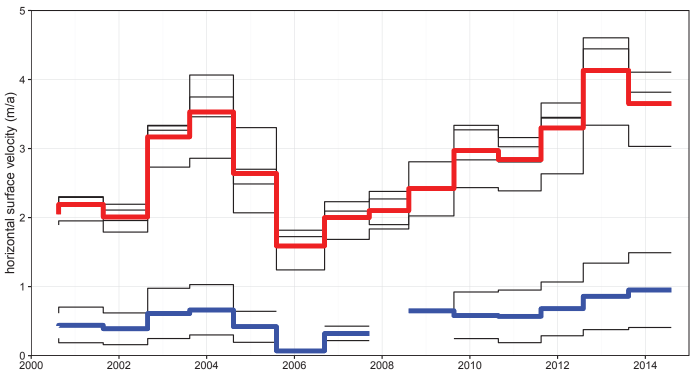

Figure A.30: Annual horizontal surface velocities at the Gemmi kinematics site for individual points and the mean of the reference points(red: 4 pts, blue: 2 pts).

Kinematics Grosses Gufer

Location: Grosses Gufer (Bernese Oberland) | Type: rock glacier | Lithology: granite

Area (km^2):	0.1
Length (m):	550
Width (m):	230
Rooting zone (m asl.):	2600
Front (m asl.):	2360
Average slope (°):	21
Exposition:	NW

Method(s): dGPS
Number of points (ref.): 83 (32)
Measurement begin: 2007
Institution: UniFR

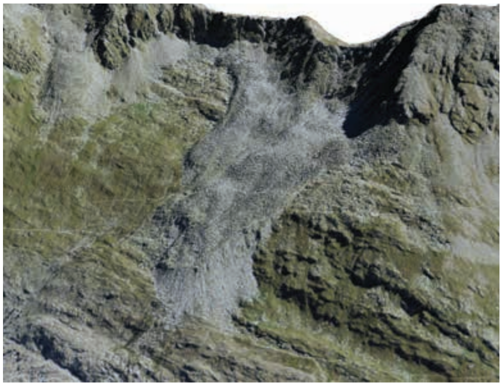

Source: Swiss Federal Office of Topography swisstopo

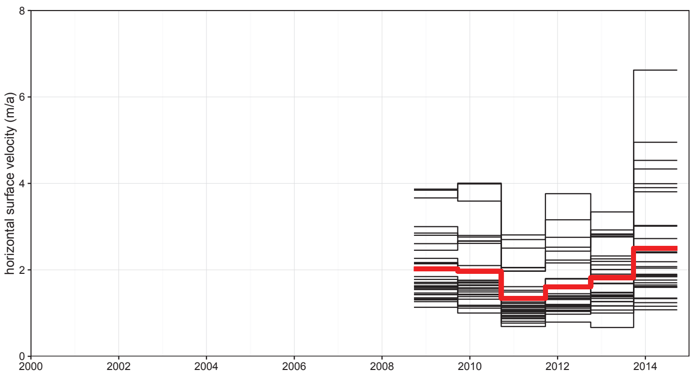

Figure A.31: Annual horizontal surface velocities at the Grosses Gufer kinematics site for individual points and the mean of the reference points (32, red line).

Kinematics Hungerlitälli 1

Location: Hungerlitaelli (Upper Valais) | Type: rock glacier | Lithology: gneiss, muscovit phyllades

Area (km^2):	0.04
Length (m):	330
Width (m):	130
Rooting zone (m asl.):	2780
Front (m asl.):	2630
Average slope (°):	26
Exposition:	NNW

Method(s): TGS (total station)
Number of points (ref.): 25 (11)
Measurement begin: 2001
Institution: UZH

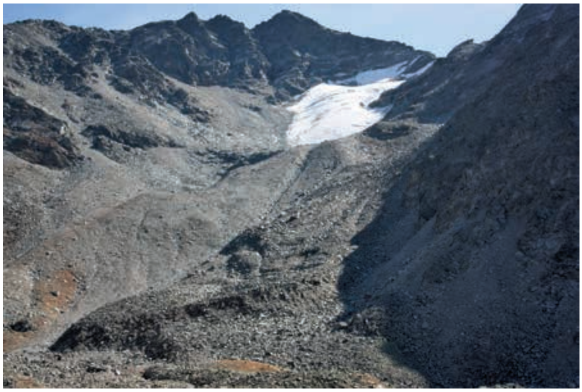

Photo: Isabelle Gärtner-Roer

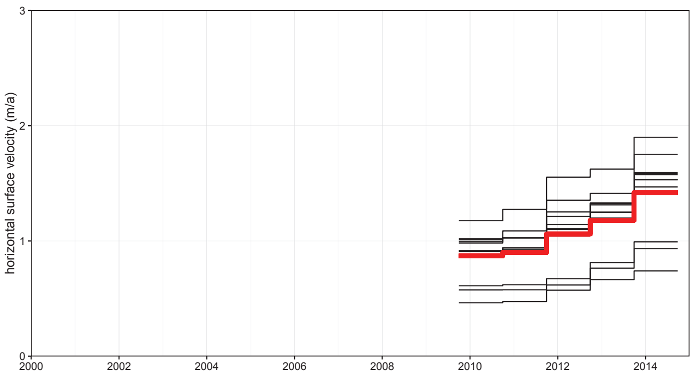

Figure A.32: Annual horizontal surface velocities at the Hungerlitälli1 kinematics site for individual points and the mean of the reference points (11, red line).

Kinematics Hungerlitälli 3

Location: Hungerlitaelli (Upper Valais) | Type: rock glacier | Lithology: gneiss, muscovit phyllades

Area (km^2):	0.04
Length (m):	310
Width (m):	140
Rooting zone (m asl.):	2650
Front (m asl.):	2510
Average slope (°):	27
Exposition:	NW

Method(s): TGS (total station)
Number of points (ref.): 31 (11)
Measurement begin: 2002
Institution: UZH

Photo: Isabelle Gärtner-Roer

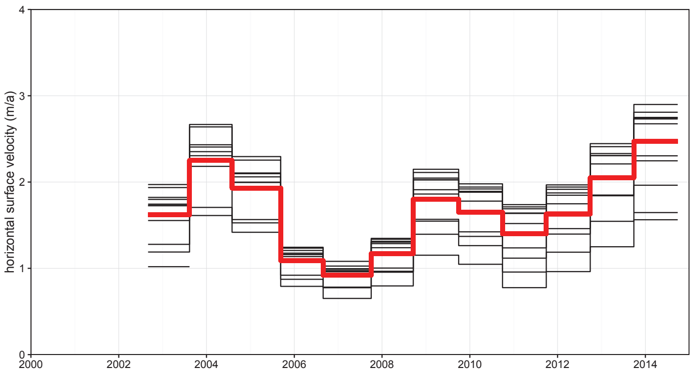

Figure A.33: Annual horizontal surface velocities at the Hungerlitälli3 kinematics site for individual points and the mean of the reference points (11, red line).

Kinematics Lapires

Location: Lapires (Lower Valais) | Type: rock glacier | Lithology: paragneiss

Area (km^2):	0.004
Length (m):	60
Width (m):	60
Rooting zone (m asl.):	2640
Front (m asl.):	2610
Average slope (°):	30
Exposition:	NNE

Method(s): dGPS
Number of points (ref.): 22 (3)
Measurement begin: 2007
Institution: UniFR

Photo: Reynald Delaloye

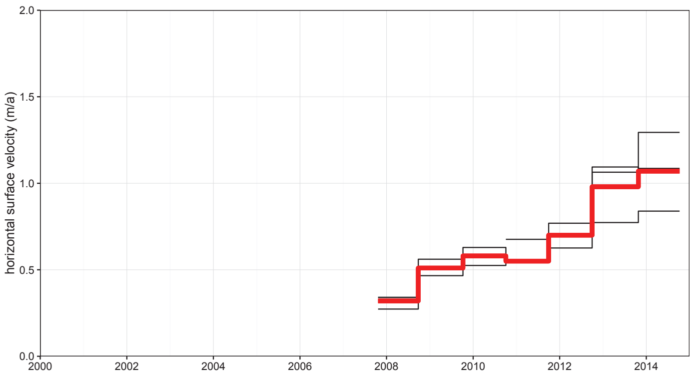

Figure A.34: Annual horizontal surface velocities at the Lapires kinematics site for individual points and the mean of the reference points (3, red line).

Kinematics Monte Prosa A

Location: Monte Prosa (Ticino) | Type: rock glacier | Lithology: granite

Area (km^2):	0.03
Length (m):	350
Width (m):	105
Rooting zone (m asl.):	2570
Front (m asl.):	2440
Average slope (°):	20
Exposition:	N

Method(s): dGPS
Number of points (ref.): 40 (11)
Measurement begin: 2009
Institution: UniFR

Source: Swiss Federal Office of Topography swisstopo

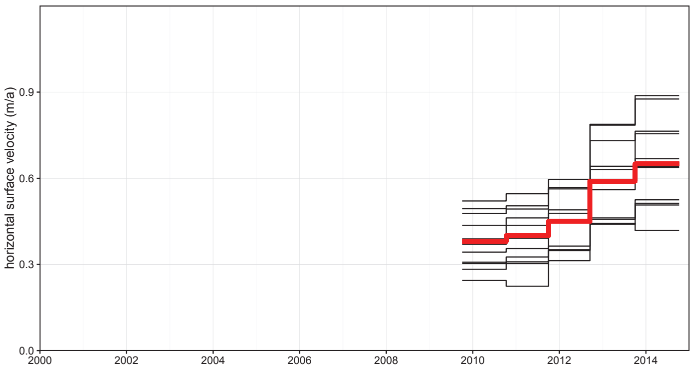

Figure A.35: Annual horizontal surface velocities at the Monte Prosa A kinematics site for individual points and the mean of the reference points (11, red line).

Kinematics Monte Prosa B

Location: Monte Prosa (Ticino) | Type: rock glacier | Lithology: granite

Area (km^2):	0.03
Length (m):	200
Width (m):	140
Rooting zone (m asl.):	2520
Front (m asl.):	2450
Average slope (°):	20
Exposition:	WNW

Method(s): dGPS
Number of points (ref.): 30 (15)
Measurement begin: 2009
Institution: UniFR

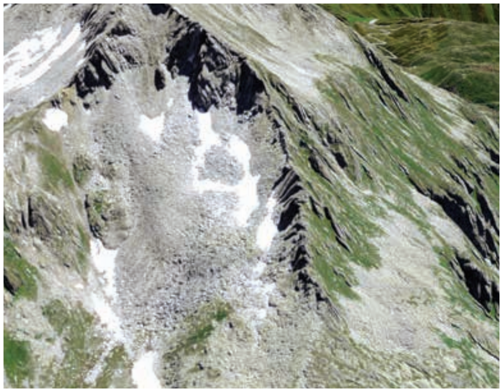

Source: Swiss Federal Office of Topography swisstopo

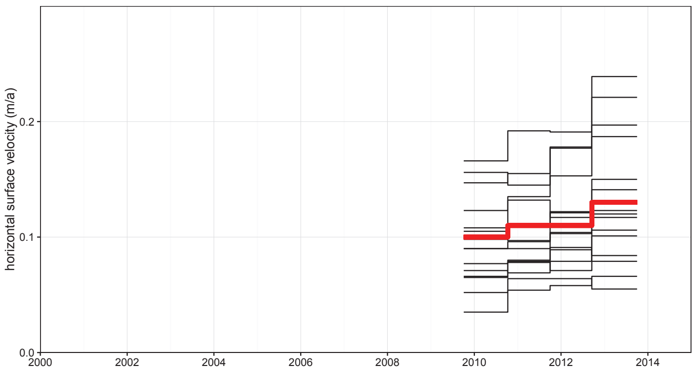

Figure A.36: Annual horizontal surface velocities at the Monte Prosa B kinematics site for individual points and the mean of the reference points (15, red line).

Kinematics Corvatsch-Murtèl

Location: Corvatsch-Murtèl | Type: rock glacier | Lithology: granite, granodiorite, greenschist

Area (km^2):	0.48
Length (m):	430
Width (m):	170
Rooting zone (m asl.):	2760
Front (m asl.):	2620
Average slope (°):	12
Exposition:	WNW

Method(s): TGS (total station)
Number of points (ref.): 11 (9)
Measurement begin: 2009
Institution: UZH

Photo: Jeannette Nötzli

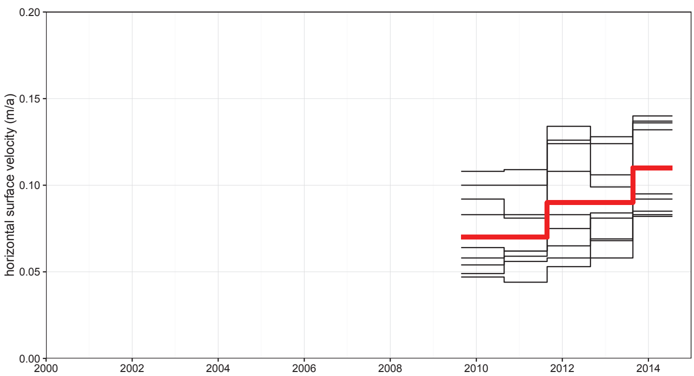

Figure A.37: Annual horizontal surface velocities at the Murtèl kinematics site for individual points and the mean of the reference points (9, red line).

Kinematics Muragl

Location: Val Muragl (Upper Engadine) | Type: rock glacier | Lithology: gneiss

Area (km^2):	0.12
Length (m):	600
Width (m):	200
Rooting zone (m asl.):	2740
Front (m asl.):	2480
Average slope (°):	14
Exposition:	NW

Method(s): TGS (total station)
Number of points (ref.): 20 (16)
Measurement begin: 2009
Institution: UZH

Photo: Isabelle Gärtner-Roer

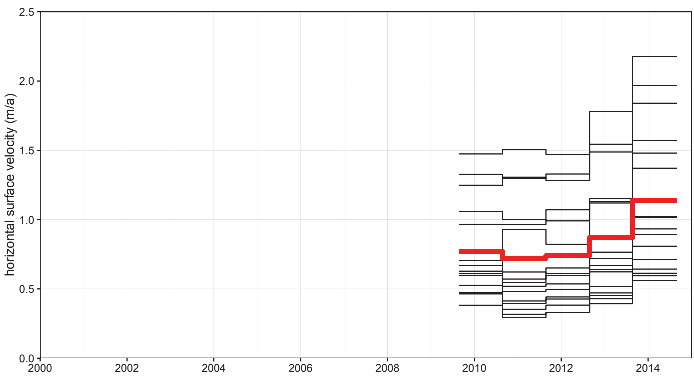

Figure A.38: Annual horizontal surface velocities at the Muragl kinematics site for individual points and the mean of the reference points (16, red line).

Kinematics Réchy

Location: Réchy (Lower Valais) | Type: rock glacier | Lithology: calc-schists

Area (km^2):	0.12
Length (m):	650
Width (m):	250
Rooting zone (m asl.):	2850
Front (m asl.):	2640
Average slope (°):	16
Exposition:	NW

Method(s): dGPS
Number of points (ref.): 215 (5)
Measurement begin: 2004
Institution: UniFR

Photo: Reynald Delaloye

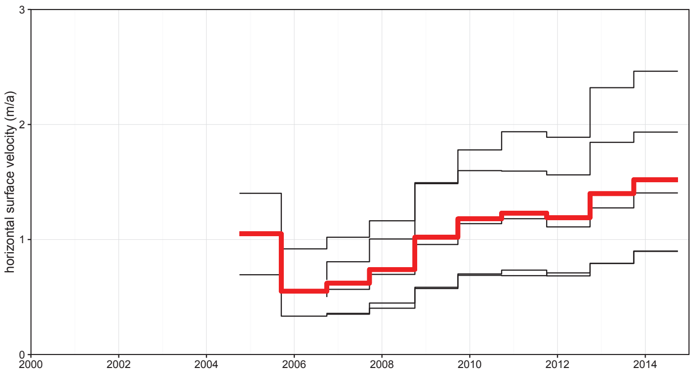

Figure A.39: Annual horizontal surface velocities at the Réchy kinematics site for individual points and the mean of the reference points (5, red line).

Kinematics Stabbio di Largario

Location: Cima di Gana Bianca (Upper Ticino) | Type: rock glacier | Lithology: two-mica granitic gneiss

Area (km^2):	0.17
Length (m):	430
Width (m):	290
Rooting zone (m asl.):	2550
Front (m asl.):	2240
Average slope (°):	21
Exposition:	N

Method(s): dGPS
Number of points (ref.): 33 (12)
Measurement begin: 2009
Institution: SUPSI

Photo: Cristian Scapozza

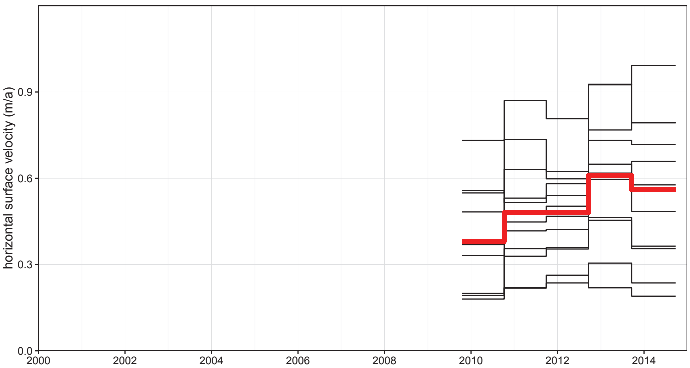

Figure A.40: Annual horizontal surface velocities at the Stabbio di Largario kinematics site for individual points and the mean of the reference points (12, red line).

Kinematics Tsarmine

Location: Val d'Arolla (Lower Valais) | Type: rock glacier | Lithology: orthogneiss

Area (km^2):	0.04
Length (m):	450
Width (m):	110
Rooting zone (m asl.):	2640
Front (m asl.):	2470
Average slope (°):	22
Exposition:	W

Method(s): dGPS
Number of points (ref.): 50 (18)
Measurement begin: 2004
Institution: UniFR/UniL

Photo: Mario Kummert

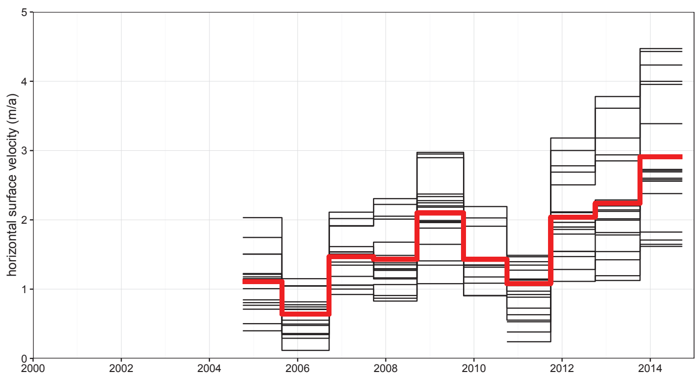

Figure A.41: Annual horizontal surface velocities at the Tsarmine kinematics site for individual points and the mean of the reference points (18, red line).

Kinematics Valle di Sceru

Location: Cima di Piancabella (Upper Ticino) | Type: rock glacier | Lithology: polycyclic paragneiss

Area (km^2):	0.06
Length (m):	210
Width (m):	145
Rooting zone (m asl.):	2550
Front (m asl.):	2450
Average slope (°):	20
Exposition:	NE

Method(s): dGPS
Number of points (ref.): 22 (19)
Measurement begin: 2009
Institution: SUPSI

Photo: Cristian Scapozza

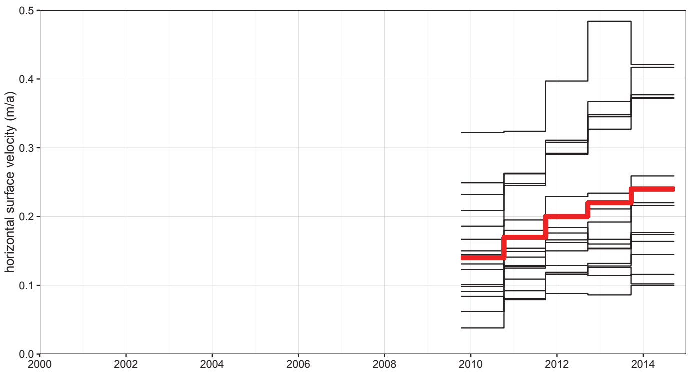

Figure A.42: Annual horizontal surface velocities at the Valle di Sceru kinematics site for individual points and the mean of the reference points (19, red line).

Kinematics Yettes Condjà B

Location: Yettes Condjà (Lower Valais) | Type: rock glacier | Lithology: paragneiss

Area (km^2):	0.02
Length (m):	270
Width (m):	80
Rooting zone (m asl.):	2720
Front (m asl.):	2600
Average slope (°):	24
Exposition:	NE

Method(s): dGPS
Number of points (ref.): 34 (17)
Measurement begin: 2000
Institution: UniL

Photo: Christophe Lambiel

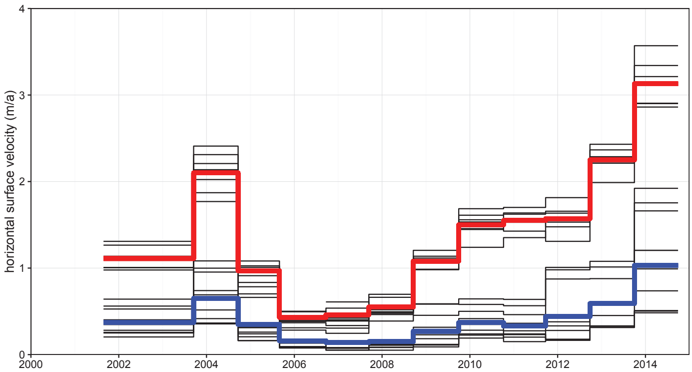

Figure A.43: Annual horizontal surface velocities at the Yettes Condjà B kinematics site for individual points and the mean of the reference points (7: red, 19: blue).

Kinematics Yettes Condjà C

Location: Yettes Condjà (Lower Valais) | Type: rock glacier | Lithology: paragneiss

Area (km^2):	0.04
Length (m):	400
Width (m):	120
Rooting zone (m asl.):	2805
Front (m asl.):	2615
Average slope (°):	25
Exposition:	NNE

Method(s): dGPS
Number of points (ref.): 34 (8)
Measurement begin: 2000
Institution: UniL

Photo: Christophe Lambiel

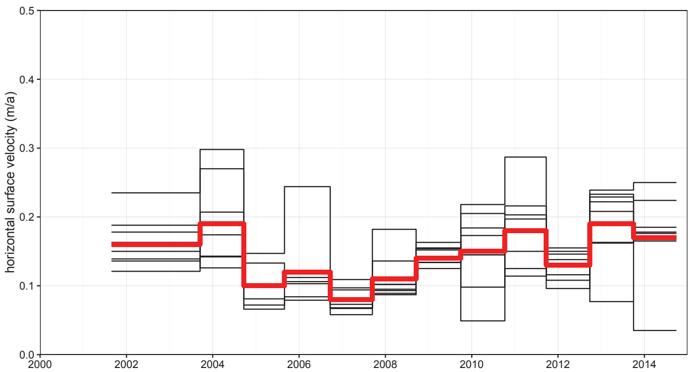

Figure A.44: Annual horizontal surface velocities at the Yettes Condjà C kinematics site for individual points and the mean of the reference points (8, red line).